

Granular Salt Summary: Reconsolidation Principles and Applications

Fuel Cycle Research & Development

Prepared for
U.S. Department of Energy
Used Fuel Disposition

Frank Hansen, Sandia National Laboratories
Till Popp, Institut für Gebirgsmechanik (IfG)
Klaus Wieczorek, Gesellschaft für Anlagen-und
Reaktorsicherheit (GRS)

Dieter Stührenberg, Bundesanstalt für
Geowissenschaften und Rohstoffe (BGR)

Sandia National Laboratories

July 2014

FCRD-UFD-2014-000590 Rev. 0



Information Only

DISCLAIMER

This information was prepared as an account of work sponsored by an agency of the U.S. Government. Neither the U.S. Government nor any agency thereof, nor any of their employees, makes any warranty, expressed or implied, or assumes any legal liability or responsibility for the accuracy, completeness, or usefulness, of any information, apparatus, product, or process disclosed, or represents that its use would not infringe privately owned rights. References herein to any specific commercial product, process, or service by trade name, trade mark, manufacturer, or otherwise, does not necessarily constitute or imply its endorsement, recommendation, or favoring by the U.S. Government or any agency thereof. The views and opinions of authors expressed herein do not necessarily state or reflect those of the U.S. Government or any agency thereof.



Sandia National Laboratories is a multi-program laboratory managed and operated by Sandia Corporation, a wholly owned subsidiary of Lockheed Martin Corporation, for the U.S. Department of Energy's National Nuclear Security Administration under contract DE-AC04-94AL85000.

Sandia Review and Approval Number: SAND2014-XXXX.

Approved for Unclassified Unlimited Release

APPENDIX E
FCT DOCUMENT COVER SHEET ¹

Name/Title of Deliverable/Milestone/Revision No. Granular Salt Summary: Reconsolidation Principles and Applications

Package Title and Number FT-14SN081805

Work Package WBS Number 1.02.08.18

Responsible Work Package Manager Kris L. Kuhlman 
(Name/Signature)

Date Submitted:

Quality Rigor Level for Deliverable/Milestone ²	<input type="checkbox"/> QRL-3	<input type="checkbox"/> QRL-2	<input type="checkbox"/> QRL-1 Nuclear Data	<input type="checkbox"/> Lab/Participant QA Program (no additional FCT QA requirements)
--	--------------------------------	--------------------------------	--	---

This deliverable was prepared in accordance with Sandia National Laboratories
(Participant/National Laboratory Name)

QA program which meets the requirements of
 DOE Order 414.1 NQA-1-2000 Other

This Deliverable was subjected to:

Technical Review

Technical Review (TR)

Review Documentation Provided

- Signed TR Report or,
- Signed TR Concurrence Sheet or,
- Signature of TR Reviewer(s) below

Name and Signature of Reviewers

Stephen Bauer 

Peer Review

Peer Review (PR)

Review Documentation Provided

- Signed PR Report or,
- Signed PR Concurrence Sheet or,
- Signature of PR Reviewer(s) below

NOTE 1: Appendix E should be filled out and submitted with the deliverable. Or, if the PICS:NE system permits, completely enter all applicable information in the PICS:NE Deliverable Form. The requirement is to ensure that all applicable information is entered either in the PICS:NE system or by using the FCT Document Cover Sheet.

NOTE 2: In some cases there may be a milestone where an item is being fabricated, maintenance is being performed on a facility, or a document is being issued through a formal document control process where it specifically calls out a formal review of the document. In these cases, documentation (e.g., inspection report, maintenance request, work planning package documentation or the documented review of the issued document through the document control process) of the completion of the activity, along with the Document Cover Sheet, is sufficient to demonstrate achieving the milestone. If QRL 1, 2, or 3 is not assigned, then the Lab / Participant QA Program (no additional FCT QA requirements) box must be checked, and the work is understood to be performed and any deliverable developed in conformance with the respective National Laboratory / Participant, DOE or NNSA-approved QA Program.

SUMMARY

Design, analysis and performance assessment of potential salt repositories for heat-generating nuclear waste require knowledge of thermal, mechanical, and fluid transport properties of reconsolidating granular salt. Ambient reconsolidation of granular salt with a small amount of accessible moisture is well understood mechanistically as buttressed by large-scale tests, laboratory measurements, and microscopic documentation of deformational processes. Permeability/density functions developed from the Waste Isolation Pilot Plant (WIPP) shaft seal experience provide a foundation for granular salt reconsolidation that informs design, analysis, or experimentation in drift sealing and backfill placement where variables are less well constrained. In contrast to significant testing and observational evidence under ambient conditions with application to shaft seal systems, large-scale salt reconsolidation under thermally-elevated or potentially dry conditions is less well described and documented.

This paper is written for stakeholders and regulators because it summarizes the scientific basis for granular salt reconsolidation, which has direct implications with respect to engineering, design, construction, evolution, and performance of lateral closure systems in a salt repository. Today's evidence supports excellent performance of sealing systems developed with crushed or granular salt. In fact, the prospect of attaining engineered performance upon completion of construction obviates reliance on modeling to argue for evolving engineering characteristics at some future time. The scientific evidence also provides a basis for modular repository design options.

Mechanical and hydrological properties of reconsolidating salt are functions of porosity which decreases as the surrounding salt formation creeps inward and compresses granular salt within the rooms, drifts or shafts. Construction circumstances within a vertical shaft provide substantial advantage for dynamic compaction techniques capable of creating high emplacement density and low initial porosity, which is an essential data point for evolutionary considerations. Placement of granular salt in a horizontal drift suffers from a less favorable construction orientation and may yield lower emplaced density and significant initial porosity for its evolutionary evaluation. In some cases, initial placement properties could be engineered to high-performance conditions by mixing crushed salt with bentonite. Drift placement of granular salt is expected to function as a low-porosity, low-permeability structural element with vital repository performance expectations. Therefore, this state-of-the-art report provides a review of the essential aspects of engineering barriers of low-porosity crushed salt, which will continue to consolidate and decrease permeability. The governing processes apply to seal design and general backfill in a horizontal configuration.

The current state of knowledge benefits from large amounts of pertinent information on granular salt reconsolidation ranging over a length scale from an atomic spacing to tens of meters. However, repository applications are concerned with very long time periods and in some cases properties of reconsolidating salt are predicted to occur far into the future after initial placement. Extrapolation based on modeling is often invoked to estimate engineering performance beyond the human experience. At the same time, the very nature of modeling introduces an element of uncertainty. Construction techniques capable of emplacing granular salt seals, perhaps with additives, to near final performance conditions greatly reduce the need for extrapolation via modeling. Much of the potential performance uncertainty can be removed by deepening the mechanistic understanding through continued research and additional validation garnered from analogues from industry practice and nature.

The science community possesses a large amount of empirical information regarding processes and characteristics associated with reduction of porosity and attendant reduction of permeability of reconsolidating granular salt. Evaporite mineral extraction often involves slurry placement to establish or enhance structural stability. The final state of the salt slurry is expected to be reconsolidated with time by the convergence process and ultimately to reach a similar mechanical stability and hydraulic resistance resident in the surrounding rock salt. The question remains as to whether the backfill of crushed salt is really compacted to a porosity of nearly zero and develops properties comparable to undisturbed rock salt. This is the crux of the technical issues addressed in this paper.

The key questions involve how, when, and to what degree properties of reconsolidating granular salt approach or attain those of the native salt formation. A vast amount of supporting data reveals the predisposition for granular salt to reconsolidate in the natural environment of deposition as well as under conditions involved with slurry injection and in situ construction techniques that may be applied in nuclear waste repositories. The key technical challenge is to draw upon the objective evidence to establish credible backfill performance and safety functions for drift seal design, analysis, and performance assessment for a salt repository.

Disaggregated salt will reconsolidate under many circumstances. Numerous laboratory studies have established parameters of the reconsolidation processes in terms of stress conditions, loading rates, temperature, access to brine or vapor, and other variables. Porosity reduction and attendant permeability decrease can be achieved via many parametric pathways. The processes by which reconsolidation accommodates removal of void space have often been evaluated in concert with standard measurements of mechanical and hydrological parameters. For example, the fundamentally important property of permeability has been measured under many conditions, most significantly as a function of porosity. Laboratory results and natural and anthropogenic

analogues support the proposition that granular salt can be reconsolidated to conditions and properties approaching or equivalent to natural, unmodified rock salt.

Fundamentals of granular salt reconsolidation are particularly relevant to establish the scientific basis for salt repository applications. Mechanistic explanations and laboratory results are available from several sources; those considered here emphasize work directly attributable to salt repository applications. Notably these include research activities associated with the WIPP in New Mexico (NM), USA and extensive contributions from research entities in Europe. Almost all crushed salt investigations in the USA centered around shaft and drift sealing operations at the WIPP site were undertaken by Sandia National Laboratories and RESPEC Inc. Similarly the research in Europe concentrated on underground gallery and borehole sealing, including the very important field test and forensics associated with Backfilling and Sealing of Underground Repositories for Radioactive Waste in Salt (BAMBUS I and II) (Bechthold et al. 1999; 2004). European research partners included

1. Bundesanstalt für Geowissenschaften und Rohstoffe (BGR), Hannover, Germany
2. Institut für Gebirgsmechanik (IfG), Leipzig, Germany
3. Gesellschaft für Anlagen- und Reaktorsicherheit (GRS), Braunschweig, Germany
4. Forschungszentrum Karlsruhe, Institut für Nukleare Entsorgung (FZK/INE), Germany
5. Groupement pour l'étude des structures souterraines de stockage (G.3S), France
6. Nuclear Research and Consultancy Group (NRG), Netherlands
7. Universitat Politècnica de Catalunya (UPC), Spain

Sandia National Laboratories joined the BAMBUS II project, which included forensics studies of the reconsolidated salt backfill. This project involved an in situ test within the Asse Mine, laboratory tests for determination of specific characteristics of the stowed crushed salt, and benchmark studies using several models, which facilitated continued development of numerical thermo-mechanical models.

In addition to the work associated with the BAMBUS investigations, reconsolidation behavior of crushed salt has been investigated by research groups in Europe and the United States (US) since the early 1980s. Contributions of the myriad working groups provided diverse approaches with slightly different emphases. Historical information, industrial experience, and analogues also provide validated practical experience and serve as extensions of laboratory-centric research efforts. These investigations have created an immense data pool comprising reconsolidation

processes and hydraulic properties, which are the most germane scientific attributes to salt repository applications.

A number of excellent research papers provide engineering characteristics and practical measurements of granular salt reconsolidation properties. Previous research contributed a comprehensive summary paper on the temporal evolution of salt reconsolidation and permeability compiled for the Vorläufige Sicherheitsanalyse Gorleben (VSG) (Popp et al. 2012a). An impressive series of papers by Spiers and co-workers (e.g., Spiers et al. 1988; 1990; Spiers and Brzesowsky, 1993) provides theory and microstructural observations of densification processes. The ongoing US/German workshops on salt repository research, design and operation include salt reconsolidation as a special focus area. Updated information on salt repository sciences including salt reconsolidation efforts can be found at the US/German workshop website http://energy.sandia.gov/?page_id=17258. Based on the considerable body of evidence densification mechanisms of both wet and dry granular salt have been well documented.

In presenting the scientific basis for granular salt reconsolidation, the case for isolation of nuclear waste in salt is bolstered. The thrust of this work pertains to seal systems constructed of crushed, mine-run, or specially conditioned granular salt; however, the behavior of the less engineered backfill is expected to evolve to the same near-impermeable end state. Several avenues of substantive evidence for reconsolidation are followed, starting with the microscopic mechanisms and observational techniques. Most laboratory results are determined at ambient conditions, although elevated-temperature reconsolidation will occur in proximity to heat-generating waste. Micromechanics also help explain field-scale testing results, which can be extended to natural and anthropogenic analogues. Practical application concerned with field-scale performance is the key point of relevance. In the end, the evidence strongly supports the proposition that granular salt will reconsolidate to low permeability associated with low porosity, as desired for long-term waste isolation in salt formations.

The purposes of this paper are to review the vast amount of knowledge concerning crushed salt reconsolidation and its attendant hydraulic properties (i.e., its capability for fluid or gas transport) and to provide a sufficient basis to understand reconsolidation and healing rates under repository conditions. The report is structured in such a way as to lead the reader to a thorough insight in the fundamental processes of crushed salt reconsolidation.

Chapter 2 summarizes deformation mechanisms and hydro-mechanical interactions during reconsolidation. An overview of investigation methodologies is given followed by examples of observational techniques. The very important influences of grain boundary fluids and fluid-

assisted deformation mechanisms are described. Documentation of reconsolidation processes is provided by examples of microstructures, including mobility of fluids in diminishing pore space.

Chapter 3 expounds on the experimental data base pertaining to crushed salt reconsolidation. Laboratory experimental methodology is described, along with representative test results. Although design, construction and performance of 100% crushed salt seals will be shown to be very favorable, these attributes can potentially be enhanced with certain engineering additives, such as clay or small volumes of water.

Chapter 4 discusses transport properties of consolidating granulated salt and provides quantitative substantiation of its evolution to characteristics emulating undisturbed rock salt. The difference between reconsolidating granular salt and the healing phenomena of damaged intact salt is also clarified. Permeability-porosity relationships are reviewed from available data sets. Finally, the impact of two-phase flow phenomena is summarized.

Chapter 5 extends microscopic and laboratory observations and data to the applicable field scale. Small-scale physics is upscaled and compared to experiences from natural or industrial analogues. The full-scale applications include the successful WIPP-shaft seal design and supporting experimental data base. The scientific basis is extended to drift-seal applications, which is likely to be a key technical issue for compartmentalizing nuclear waste repositories in salt. The BAMBUS experience is enormously valuable in the drift-seal context. Finally, the introduction of further commercial mining experiences helps strengthen the argument that reconsolidation of granular rock salt can be achieved with modest engineering investment.

Various constitutive models describing crushed salt reconsolidation have been developed from purely empirical types to models that distinguish between different deformation mechanisms. Although in some places simulation results are mentioned, describing these models and their calibration procedure is beyond the scope of this report, which concentrates on the principles of reconsolidation processes and extension of this fundamental understanding to salt repository applications.

Given the depth and breadth of the science behind salt reconsolidation, what remains to be done? The final chapter provides a look forward to research in the laboratory that is intended to address perceived uncertainties. In addition, field examples and forensic investigations continue to provide substantiation of performance over a full-scale repository application.

ACKNOWLEDGEMENTS

Authors of this document are indebted to Laura Connolly of Sandia Labs, who persevered through many iterations of review and input from the international authors. This summary of the state of the art in granular salt consolidation is testimony to excellent international collaboration.

TABLE OF CONTENTS

SUMMARY	iii
ACKNOWLEDGEMENTS	ix
TABLE OF CONTENTS	ix
LIST OF FIGURES	x
LIST OF TABLES	xii
ACRONYMS	xiii
1 INTRODUCTION	1-1
2 MICROMECHANICS – HYDRO-MECHANICAL INTERACTIONS	2-2
2.1 Overview / Methodology	2-2
2.2 Deformation mechanisms – dry/wet conditions	2-6
2.3 Deformation mechanisms—temperature effects	2-10
2.4 Hydromechanical interactions	2-12
3 EXPERIMENTAL SALT RECONSOLIDATION MECHANICS	3-1
3.1 Experimental methodology	3-1
3.1.1 Experimental results	3-6
3.1.2 Improvement of the compaction behavior – role of additives	3-12
4 TRANSPORT PROPERTIES OF COMPACTED CRUSHED SALT	4-1
4.1 Methodology	4-1
4.2 Permeability/porosity relationships – natural rock salt vs. compacted crushed salt	4-1
4.3 Impact of two-phase flow phenomena	4-3
4.4 Results from laboratory testing with a crushed salt / clay mixture	4-7
4.5 Transport properties of compacted crushed salt - synthesis	4-8
5 NATURAL ANALOGUES / FIELD-SCALE OBSERVATIONS / APPLICATIONS	5-1
5.1 Introduction	5-1
5.1.1 Anthropogenic analogues	5-1
5.1.2 Technical analogues	5-2
5.1.3 Healing and sealing the EDZ	5-2

5.1.4	Geologic analogues	5-2
5.1.5	Underground Research Laboratories (URL's)	5-3
5.1.6	WIPP Shaft Seal	5-5
5.2	Drift closure	5-9
5.2.1	BAMBUS II – mockup-test	5-9
5.2.2	Operating Mines - Crushed salt properties and microstructural observations	5-12
5.2.3	Convergence - Drift closures at WIPP	5-14
5.2.4	Preliminary safety analysis Gorleben (VSG)	5-15
6	PERCEPTIONS / FUTURE WORK	6-1
7	REFERENCES	7-1

LIST OF FIGURES

Figure 2.1	Deformation mechanisms in crushed salt; humidity-induced processes are blue shaded	2-4
Figure 2.2	Consolidated granular salt forensic sample preparation	2-5
Figure 2.3.	Changes in fabric during compaction of crushed salt	2-7
Figure 2.4 a)	Grain boundary diffusional pressure mechanism and b) plasticity-coupled pressure mechanism with plastically-deformed region shaded	2-9
Figure 2.5	WIPP Room B heater with reconsolidated salt caked on the circumference	2-10
Figure 2.6	Extensive grain deformation during reconsolidation at 250°C plasticity coupled pressure solution a), and polygonization b)	2-12
Figure 2.7	Schematic drawings showing the dihedral angle and its significance for connectivity of fluids in texturally equilibrated porous rocks	2-14
Figure 2.8	Schematic of fluid redistribution in granular aggregates during compaction	2-15
Figure 2.9	Relationship between gas permeability and the Biot-coefficient for dilated rock salt	2-17
Figure 3.1	Experimental reconsolidation set-ups	3-2
Figure 3.2	Compaction of crushed salt – schematics of experimental procedures	3-4
Figure 3.3	Consolidation behavior of granular backfill investigated under oedometer test conditions	3-5
Figure 3.4	Consolidation tests of type II – creep tests: a) oedometer test on dry crushed salt, b) isostatic creep consolidation tests on dry and wet salt bricks	3-8
Figure 3.5	Ongoing multistep oedometer tests at GRS	3-9
Figure 3.6	Triaxial compaction test TK-031	3-10
Figure 3.7	Comparison of volumetric strain rates at 50°C. Triaxial compaction test TK-031 and oedometer test Oedo-049	3-12
Figure 3.8	Impact of additives on the compaction behavior of crushed salt	3-14
Figure 4.1	Permeability-porosity relations of dilating rock salt and reconsolidating granular salt	4-3

Figure 4.2 Two-flow-phase phenomena in crushed salt. a) Relative permeability functions predicted by various models (Cinar, 2000). b) Plot of gas threshold pressure vs. intrinsic permeability 4-6

Figure 4.3 Transport properties of crushed salt/clay aggregates using gas a) and brine b) 4-8

Figure 4.4 Synoptic view of permeability-porosity data sets for crushed salt aggregates 4-9

Figure 5.1 Summary of analogues 5-3

Figure 5.2 Volumetric Strain and Brine Flow Measurements on Reconsolidating Granular Salt 5-8

Figure 5.3 Dynamically compacted WIPP salt (left), reconsolidated WIPP salt (right) 5-9

Figure 5.4 Photograph of the BAMBUS II re-excavation 5-10

Figure 5.5 Micro-structures of consolidated Salt with 20.7% Porosity 5-12

Figure 5.6 Reconsolidation of slurry backfill at the K2 mine after 30 years 5-13

Figure 5.7 Closure measurements Panel 1 entry 5-15

DRAFT

LIST OF TABLES

Table 5.1. Underground research labs in salt formations with backfilling investigations5-5

DRAFT

ACRONYMS

μCT	Micro-Tomography
3D	Three-Dimensional
BAMBUS	Backfilling and Sealing of Underground Repositories for Radioactive Waste in Salt
Cryo-SEM	Cryogenic-Scanning Electron Microscope
FZK/INE	Forschungszentrum Karlsruhe, Institut für Nukleare Entsorgung
G.3S	Groupement pour l'étude des structures souterraines de stockage
GRS	Bundesanstalt für Geowissenschaften und Rohstoffe
IfG	Institut für Gebirgsmechanik
GRS	Gesellschaft für Anlagen-und Reaktorsicherheit
NM	New Mexico
NRG	Nuclear Research and Consultancy Group
REPOPERM	Restporosität und permeabilität von kompaktierendem Salzgrus-Versatz (Residual porosity and permeability of compacting granular salt backfill)
SEM	Scanning Electron Microscope
TSDE	Thermal Simulation of Drift Emplacement
UPC	Universitat Politecnica de Catalunya
URL	Underground Research Laboratory
USA	United States of America
VSG	Vorläufige Sicherheitsanalyse Gorleben
WIPP	Waste Isolation Pilot Plant

1 INTRODUCTION

Reconsolidation of granular salt has long been recognized as a key scientific issue in salt repository applications. In addition to mechanical and thermal properties, the most essential phenomena pertain to permeability as a function of porosity. The fact that disaggregated salt can be reconstituted to characteristics equivalent to native salt has been widely demonstrated. However, for repository applications, the overriding concern is how soon under variable conditions does reconsolidating salt attain desirable performance characteristics. This paper summarizes the abundant information on this topic, from first principles to full-scale applications and analogues.

Presentation of material in this document generally progresses from small to large scale. The physics of reconsolidation at the micro-scale has been extensively studied. The initial portions of this review describe mechanisms of reconsolidation from large void fractions to low porosity. The most important region of interest pertains to the reduction of permeability as connected porosity is eliminated. Pressure solution and re-precipitation provide the solution transfer that affects the fundamental material behavior.

Salt reconsolidation mechanics have been investigated by means of several experimental procedures over time, with increasing sophistication and accuracy. Improvements in techniques as well as test-to-test comparisons have illuminated a more complete understanding of the scientific evidence than heretofore appreciated. The all-important regimes of low strain rates and low stress magnitudes have been explored in numerous lab experiments. Presence of small amounts of moisture greatly facilitate the consolidation process. Interpretation of the effects of temperature, stress, moisture and test techniques are vital to the application of laboratory results.

The applications emphasized here pertain to seal systems and backfill within salt repositories for nuclear waste, which embody large-scale construction and long-term performance. Analogues provide useful long-term, full-scale anecdotal information, which confirm reconstitution of granular salt or slurry to low porosity low permeability states. In repository applications, timing of attainment of performance specifications is key to meeting regulatory requirements. Additives such as moisture and clay improve placement properties of engineered structures and ensure both early and long-term performance.

Crushed or granular salt reconsolidation will play an important role if a salt formation is selected for permanent isolation of nuclear waste because in the salt disposal concept crushed salt is the

most suitable backfill material. Crushed salt is readily compacted and reconsolidated. The thermal, mechanical and chemical properties of reconsolidated granular salt can be constructed to rapidly approach those of the undisturbed surrounding rock salt. Reuse of mined salt in the underground facility provides operational efficiency, reduces hoisting and optimizes material transport. Depending on the closure concept of the respective repository the main backfill functions are

- to act as a long-term barrier against inflowing brine or water and to eliminate release pathways via drifts and shafts
- to conduct the heat generated by radioactive decay from the waste to the host rock
- to stabilize the repository excavations
- to provide low permeability and/or diffusivity and/or long-term retardation

The remainder of this report provides technical information regarding characteristics pertaining to these functions.

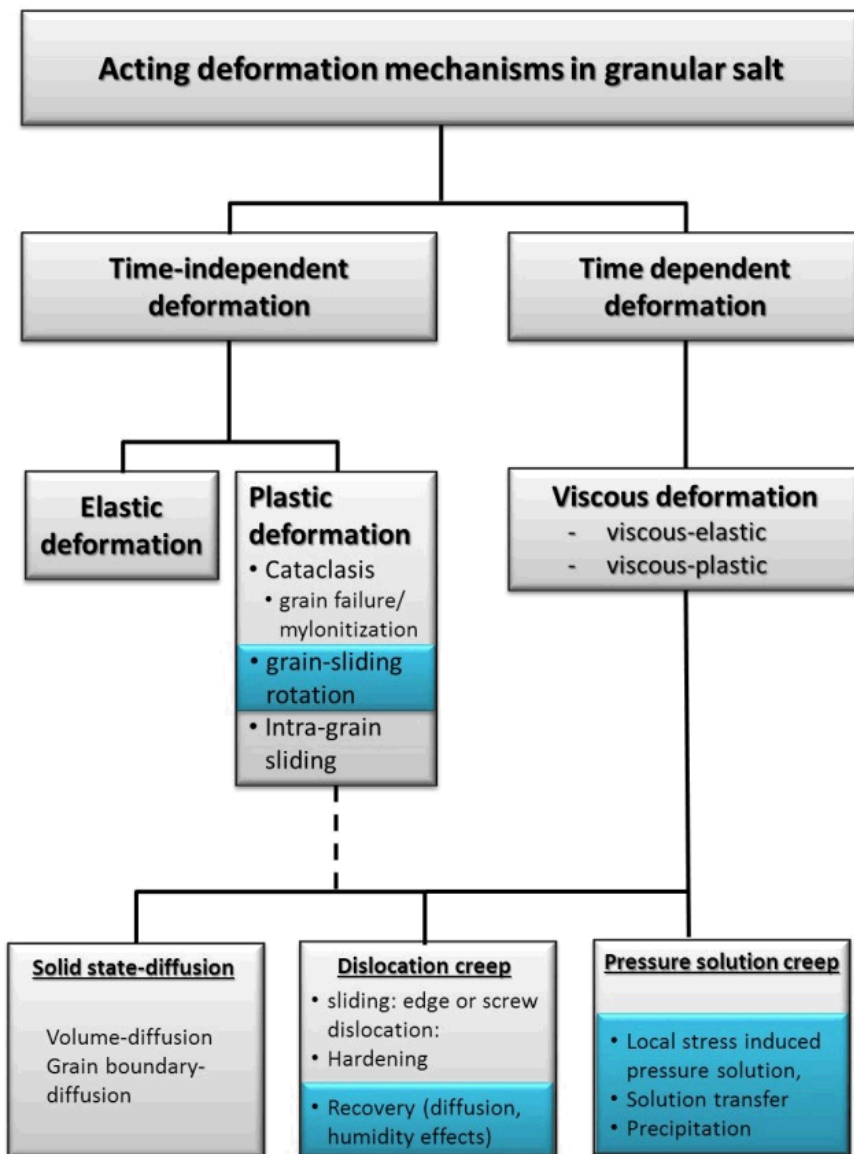
2 MICROMECHANICS – HYDRO-MECHANICAL INTERACTIONS

2.1 Overview / Methodology

Several processes can account for deformation, compaction, and consolidation of granular material. At the outset it is important to acknowledge that both natural and laboratory deformation and compaction of aggregates is a function of multiple simultaneous processes. The degree to which each process contributes to the consolidation phenomenon depends on the extent of consolidation already imparted to the volume of interest. **Figure 2.1** illustrates deformation processes in series and in parallel that may influence reconsolidation of granular salt. Dynamic compaction, as might be employed during construction, removes void space by instantaneous cataclastic fracture processes. Plasticity of individual grains becomes an essential mechanism as porosity becomes smaller and smaller. Fluid-aided processes highlighted in blue on **Figure 2.1** are effective at low porosity and are the primary, late-stage mechanisms that complete the transition from a porous material to the equivalent of an intact solid. Overall, the effective reconsolidation processes can be influenced by primary factors of moisture content, temperature, applied stress, initial porosity, and grain size. Other factors viewed as less important than the primary factors include grain size distribution, impurity content, cycle of load path, and brine chemistry (e.g., Davidson and Dusseault, 1996).

The granular salt material used for backfill applications can have a significant grain size variation depending on the manner of production or by engineering a particular grain-size distribution. The effects of grain size on compaction are certainly reduced if the construction method includes dynamic compaction. Without added construction effort, a proper gradation of particles with a distribution of sizes appears to produce the lowest porosity because finer particles fill voids between larger grains. It is interesting to note that porosity decrease increases with increasing maximum particle size. This observation can be explained by comminution of larger salt particles into small particles, which fill voids. In addition, inhomogeneous grain size distributions allow easier deformation by particle sliding and rearrangement under early stages of reconsolidation.

Consolidation deformation mechanisms involving dislocation motion, as shown in **Figure 2.1**, are the same as those that govern during deformation of intact rock salt. Air contained in the void space at high porosity is squeezed out during reconsolidation. It has been postulated that as permeability decreases with progressive consolidation local pore-fluid pressure could develop and may hinder a complete pore space closure.



Note/Source: (modified after Elliger, 2004)

Figure 2.1 Deformation mechanisms in crushed salt; humidity-induced processes are blue shaded.

Identification of acting deformation mechanisms can be inferred from microstructural observations made with optical and electron microscopes on fragments of a tested specimen, polished thin sections, or etched cleavage chips. Mechanically compacted observational specimens are prepared *post facto*, typically as shown in **Figure 2.2**. The consolidated sample is cut in half length-wise using a low-damage diamond wire saw and subsequently quartered. Optical slides are

conveniently prepared from these sawn sections, as shown on the right in **Figure 2.2**. The blue color is low-viscosity epoxy drawn into the void space by vacuum. The quarter-round subsections can be broken by hand to expose a surface of the compacted material. These fresh surfaces are often sputter-coated and examined using a Scanning Electron Microscope (SEM). In some cases individual grains can be plucked, cleaved, etched and examined.



Figure 2.2 Consolidated granular salt forensic sample preparation.

Observational methods include optical microscopy on 5-mm thick petrographic sections and etched cleavage chips. SEM techniques can be used to examine freshly broken surfaces and coated petrographic sections. The relatively thick petrographic section allows optical observations on the surface, along grain boundaries and through the crystal structure. Renard et al. (2004) successfully visualized pore space changes in halite aggregate samples during time-dependent compaction using three-dimensional (3D) X-ray micro-tomography (μ CT). This new technique provides 3D data that allow an estimate of the transport properties of the samples by modeling transport properties of the observed pore space network. Direct observations of fluid-filled grain boundaries can be obtained by using the cryogenic-scanning electron microscope (cryo-SEM) in which the grain boundary fluids were frozen before breaking the samples (e.g., Schenk et al. 2006). This gives additional information about the presence of brine which strongly

affects the microstructural evolution and the mechanical and transport properties of compressed salt.

The following paragraphs summarize the microstructural processes and complex hydro-mechanical interactions during granular salt reconsolidation. This information provides the fundamental underpinnings for describing the evolution of the crushed salt seal element from a porous material into the equivalent of an impermeable solid.

2.2 Deformation mechanisms – dry/wet conditions

Mechanisms of salt densification have been extensively described in the literature as cited throughout. As illustrated in **Figure 2.1**, micromechanical processes depend on many external boundary conditions and extant internal conditions. For the intended function as seal elements in a salt repository, multiple parameters converge to only a few key considerations: these include water content, porosity, deformation rate, and temperature. Under in situ conditions, the convergence of the mine openings (drifts or shafts) provides the driving boundary condition for the operative processes. Material properties of the consolidating mass are inextricably tied to the inward creep of the native formation. Granular salt reconsolidation results from time-dependent deformation processes in the surrounding salt. The convergence itself is influenced by reduction of the backfill porosity and attendant stress increase in the backfill.

The initial porosity of a disaggregated natural geomaterial, including salt, is usually between 30 and 40%. Unconsolidated piles of salt are held in a natural angle of repose by grain-to-grain contact as can be seen on the left side of **Figure 2.3**. The broken material appears rectangular owing to near-perfect cleavage and the angular grains rest with their tips on neighboring grains forming a loose aggregate. The starting material pore space and aggregate characteristics can be readily modified by construction methods, including dynamic compaction.

The consolidation sequence proceeds thusly: Processes at high porosity involve instantaneous grain rearrangement (e.g., grain sliding and rotation) and cataclasis (brittle failure of grains due to local stress concentrations or frictional slip), which can proceed only so far before grain boundary processes and crystal-plastic mechanisms begin to dominate further porosity reduction. This microstructural crushed salt sequence is shown on the left side of **Figure 2.3** (revised after Spangenberg, 1998). The right side of **Figure 2.3** is a 3D X-ray μ CT. The μ CT images in a) show two grains of halite before (left, initial aggregate) and after (right, 11% deformation) indentation by pressure solution. The arrows indicate the indentation of grain h1 into grain h2. The pore space (p) appears darker. The μ CT images in b) are extractions of the pore surface on two sub-volumes showing that the preceding grain contact has disappeared and healing has occurred (Renard et al. 2004).

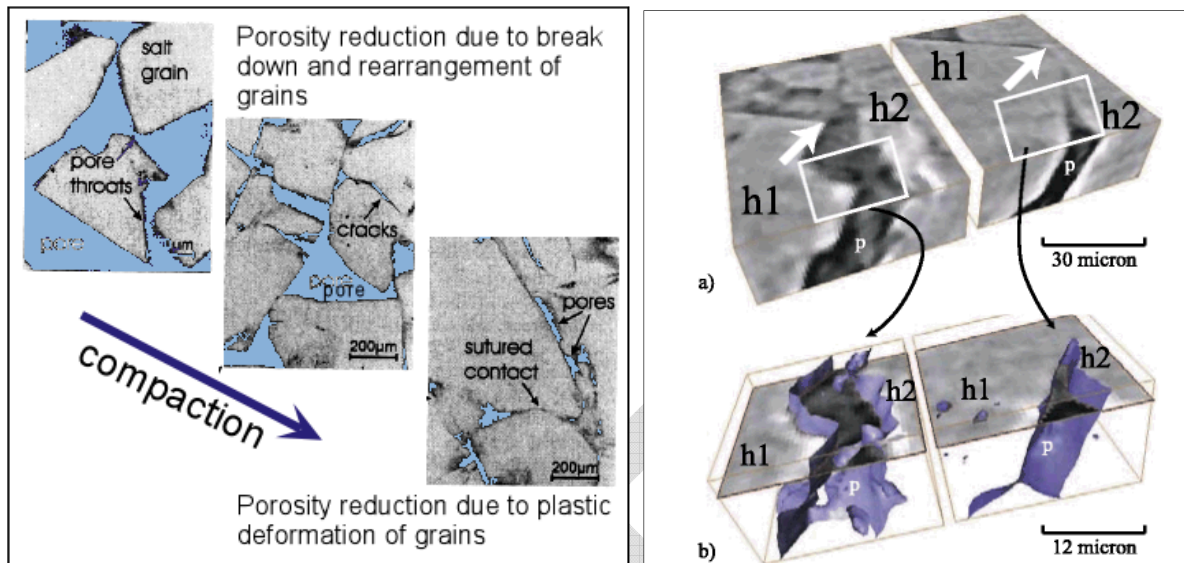


Figure 2.3. Changes in fabric during compaction of crushed salt.

As porosity is reduced, plastic deformation proceeds, including dislocation motion accommodated by glide and cross slip along the dodecahedral $\{110\}$ planes. Salt plasticity promoted by these mechanisms has been well documented in many laboratory tests on intact salt (e.g., Hansen, 1985). Similar deformational mechanisms are less frequently observed in reconsolidated samples because tests taken to $<10\%$ porosity are scarce and observational microscopy has not been routinely performed. Additionally, because a thin water film is ubiquitous along grain boundaries, fluid-assisted creep deformation mechanisms will contribute to the time-dependent densification mechanisms. As the plastic mechanisms change the shape of the grains and dissolution-precipitation processes operate along the grain boundaries, the geometry of the pores will be strongly modified as indicated in Figure 2.3 (right side).

The complexity of deformation mechanisms are illustrated by previous microstructural studies, e.g., Spiers and Brzesowsky (1993). They indicated that

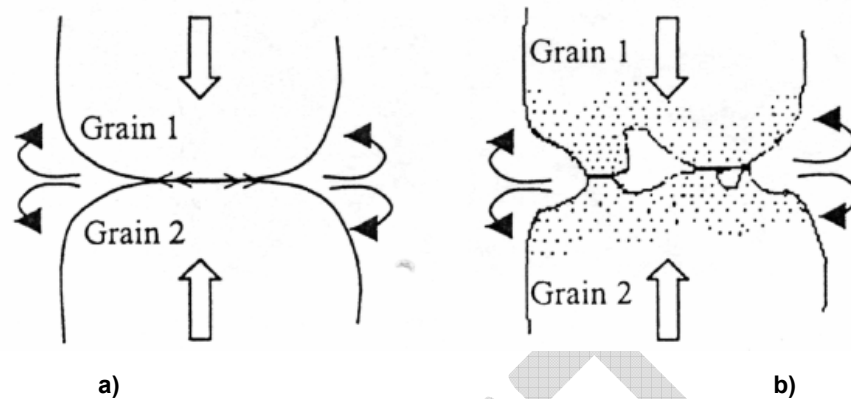
- significant differences in microstructure were observed between samples tested at high and low stresses
- wet material densified at stresses below 5 MPa, abundant grain-to-grain indentations and contact truncations were observed, and little evidence was found in these samples for plastic deformation or for marginal dissolution or undercutting at grain contacts
- occasional evidence was found for grain boundary migration and contact cataclasis in highly compacted samples tested at 4.2 MPa

- in the wet-densified samples tested at 6-8 MPa microstructures and overgrowths were widely developed in the pores

Because pressure-solution creep is considered to be an important mechanism of crushed salt compaction, it warrants additional description here. Comprehensive reviews regarding the fundamental processes of mechanisms, thermodynamics and models of pressure solution are given elsewhere (e.g., Hellmann et al. 2002, Spiers and Brzesowsky, 1993). Experimental approaches focusing on pressure solution during the deformation of unconsolidated crushed salt aggregates have been described by several authors (e.g., Raj, 1982; Urai et al. 1986a, b; Spiers et al. 1990; Spiers and Brzesowsky, 1993; Hellmann et al. 1998). In salt aggregates where the solid grains are plastically deformable, two types of pressure solution densification mechanisms are possible:

- grain boundary diffusional pressure solution
- plasticity-coupled pressure solution

The driving force for pressure solution in a granular aggregate is related to stress variations along the grain surface (Paterson, 1973). **Figure 2.4 a)** presents a sketch of pressure solution as it occurs in response to a non-zero effective stress, i.e., the normal stress component across a grain contact is greater than the stress on the free pore surface of the same grain. Thus, the chemical potential can be seen to vary along the surface of a grain, driving a diffusive flux of solutes from the contact area to the free pore surface. The high stress at grain contacts causes dissolution of the minerals at the grain boundary, transport of the dissolved material in a fluid phase out of the grain boundary and precipitation of this material in the pore space on the less stressed faces of the grains. Additional driving force (chemical potential drop) both along and across grain boundaries can be provided by internal plastic deformation of the grains, giving rise to combined grain boundary migration and solution-precipitation creep as illustrated in **Figure 2.4 b)**. The relative importance of each process depends on variables such as temperature, confining pressure, grain size, solid solution impurities, second phase content, and most strongly on the presence of sufficient water at grain boundaries to enable solution-precipitation phenomena.



Note/Source: (after Spiers and Brzesowsky, 1993)

Figure 2.4 a) Grain boundary diffusional pressure mechanism and b) plasticity-coupled pressure mechanism with plastically-deformed region shaded.

These investigations found that without the added moisture during compaction of the crushed salt the importance of the diffusional creep mechanism would diminish. If moisture is available in the contact area, even very small amounts are sufficient to activate pressure solution processes characterised by material dissolution and reprecipitation. In addition, fluid assisted grain boundary migration is an efficient process of reducing dislocation density and hence removing the stored energy of dislocations, even at room temperature. Thus the grain boundary diffusional pressure mechanism dramatically enhances the densification rate in the crushed salt (Spiers et al. 1990; Callahan et al. 1996; 1998).

In summary, because the above described processes have been documented in laboratory experiments on natural and artificial salt aggregates and in deformed natural salt, they can be attributed as a fact, i.e., ambient reconsolidation of granular salt with a small amount of moisture is well understood mechanistically as underpinned by large-scale tests, laboratory measurements, and microscopic documentation of deformational processes. Empirical evidence indicates that fluid-aided processes will be operative in typical bedded salt as porosity reduces below 10%, even if no construction moisture is added. Nominally, domal salt contains much less moisture than bedded salt, so enhanced compaction and reconsolidation may be facilitated by addition of small amounts of water during construction. As cited throughout this paper, observations concerned with bedded salt show adequate moisture from negative crystals, grain boundary fluid and hydrous minerals to sustain fluid-assisted processes.

2.3 Deformation mechanisms—temperature effects

Small volumes of granular salt may experience significantly elevated temperatures in repositories for heat-generating nuclear waste. High temperature compression would be expected around the waste package, especially if borehole emplacement is used and crushed salt is placed in the annulus. If the thermal load is high (i.e., $\sim 20 \text{ W/m}^2$) and closure is rapid, backfill salt may also experience reconsolidation at elevated temperature. **Figure 2.5** is an example of reconsolidation of granular salt around a heater from experiments conducted in the WIPP facility. Heaters were placed vertically into the floor and the annulus was loosely filled with salt aggregate. After the tests were terminated, some of the heaters were removed by overcoring; the reconsolidated salt rind and the heater are shown the photograph in **Figure 2.5**.



Figure 2.5 WIPP Room B heater with reconsolidated salt caked on the circumference.

To further the understanding of reconsolidation under elevated temperature, initial experimental work was undertaken in the US, including laboratory studies, modeling and microscopy (Hansen et al. 2012, Broome et al. 2014). In the laboratory, mine-run salt from the Waste Isolation Pilot Plant (WIPP) was first dried at 105°C until no further weight loss occurred. Vented samples were placed in a pressure vessel and maintained at test temperatures of 100, 175 or 250°C . In hydrostatic tests, confining pressure was increased to 20 MPa with periodic unload/reload loops implemented to determine bulk modulus. Volume strain increased with increasing temperature. In shear tests, axial stress was superimposed so that the granular salt was subjected to a differential

stress. As axial load was applied, periodic unload/reload loops were conducted and used to determine elastic modulus and lateral strain ratio. At predetermined differential stress levels, conditions were held constant to measure creep reconsolidation. At these test conditions the creep rate (rate of deformation under constant stress) increased with increasing temperature and increasing stress and decreased as porosity decreased.

Microstructural observations were made on several of the reconsolidated granular salt specimens deformed at 250°C under hydrostatic-quasistatic, shear-quasistatic, and creep conditions. Most test specimens were consolidated from ~40% to ~10% porosity, with a few tests taken to porosity less than 5%. Porosity was estimated from microscopic point-counting techniques and mechanical test data. Extensive grain deformation was exhibited in the final, low porosity states. As with ambient tests, initial porosity was removed by grain boundary sliding with attendant comminution at grain contacts. Widespread crystal plasticity was manifested in elongated and sinuous grain fabric. Etching techniques highlight heavily deformed grains that exhibit wavy slip band microstructures, and climb recovery processes with an associated minute subgrain size. Free dislocation density was sparse in the highly deformed grains. Despite chaotic substructure appearance, which could be related to potentially high internal strain energy, only minor dynamic recrystallization was observed. Notwithstanding drying the granular salt to a typically accepted “dry” condition, sufficient brine apparently remained within the crystal lattice as fluid inclusions to facilitate fluid-assisted diffusional transfer.

Figure 2.6 shows SEM photomicrographs of consolidated granular salt in which crystal deformation has occurred. Photomicrograph 2.6 a) was taken of an etched thick-thin section prepared from granular salt reconsolidated to low porosity at 250°C. Smaller grains in the center of the image exhibit extremely small subgrains indicative of high stress difference (Carter et al. 1982). Crystal elongation facilitated by slip on {110} planes apparently also carries internal fluid inclusions to the grain boundaries. The fluid thereby made available to the grain boundary promotes pressure solution and consumption of the fine grains. The smaller grains in **Figure 2.6 a)** would soon be consumed by solution transfer driven by gradients in chemical potential associated with strain gradients developed between grain contacts and pore walls (Spiers and Brzesowsky, 1993). Under these conditions at low porosity the densification processes involve plasticity coupled pressure solution.

Figure 2.6 b) illuminates a crystal of salt that was subject to reconsolidation at 250°C. A single grain was cleaved, etched, sputter coated, and examined by the Scanning Electron Microscope (SEM). Etch techniques highlight the internal crystal structure, which comprises equant subgrains as a result of crystal plasticity via polygonization. The right image at higher magnification exhibits well-developed subgrains indicative of thermally activated climb recovery within the

crystal. In addition, the free-dislocation density within the polygons is very low, indicating extensive recovery by climb. Based on previous research summarized by Carter et al. (1982) deformed salt substructure displays a relationship between the applied steady state stress difference and subgrain size. The average subgrain size in this micrograph (and others) is approximately 25 μm , which according to Carter et al. (1982) equates to a stress difference of roughly 7 MPa, the maximal differential stress of the test.

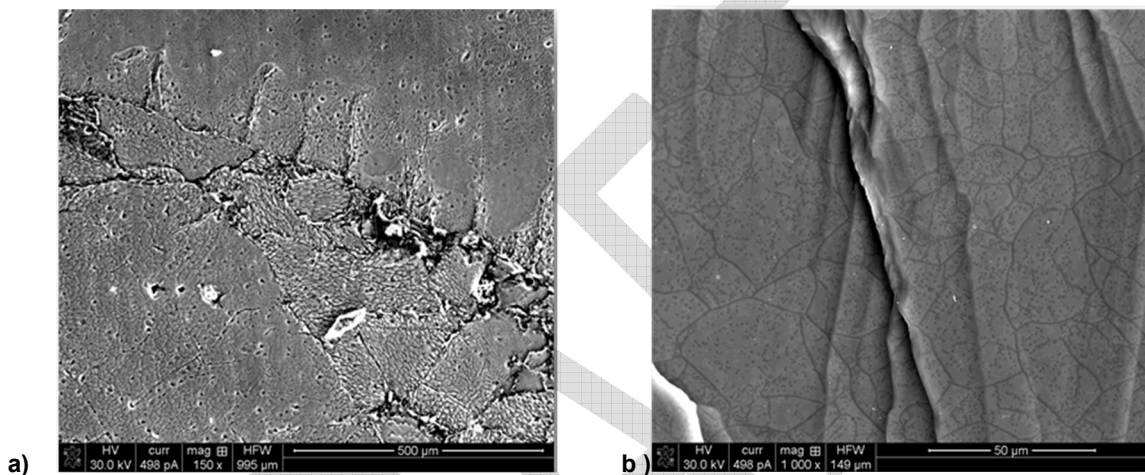


Figure 2.6 Extensive grain deformation during reconsolidation at 250°C plasticity coupled pressure solution a), and polygonization b).

In summary, reconsolidation at elevated temperature and low porosity appears to include extensive glide that enables considerable grain distortion. As bedded salt is deformed under these conditions fluid inclusions are translated to the grain boundary to affect pressure solution. Internal strain of reconsolidating grains is recovered by thermally activated climb and polygonization. Reconsolidation of granular salt in a high temperature regime would be locally important in the vicinity of a heat-generating waste package. The limited experimental and observational work presented here reveals extensive reconsolidation by plasticity-aided pressure solution that consumes smaller grains accompanied by climb-controlled crystal plasticity within larger grains.

2.4 Hydromechanical interactions

One of the key technical issues concerning properties of reconsolidating granular salt is the mobility of fluids in the residual pore space. It is well known from nature and laboratory experiments that small amounts of residual brine will be present at grain boundaries in granular salt. Intact salt grains exhibit thin fluid films with a thickness of a few nanometers, which can be

seen under the microscope as channels or pores. Grain boundary structure is believed to change during dynamic recrystallization in presence of fluids, such that grain boundary migration is assisted by thin fluid films residing on the grain boundaries (Urai et al. 1986b; Drury & Urai, 1990). In addition to mechanical aspects, the distribution and mobility of water existing inside the pore space may play an important role with respect to safety-assessments of salt repositories. The quantity of accessible moisture controls the volume of water available for corrosion. As described above, a minute amount of moisture on the grain boundaries has a first-order effect on reduction of residual porosity.

Two aspects are of primary importance in the complex hydro-chemical-mechanical interactions:

- advective release of moisture and/or
- retention, which may impede the consolidation process by developing pore pressure

The presence of brine strongly affects microstructural evolution and the mechanical and transport properties of the material (e.g., Schenk et al. 2006), although the structure of the halite grain boundaries which contain water is still a matter of debate. One model proposes a thin fluid film transmits the contact stress, therefore diffusion transports dissolved material. On the other hand, the thin film fluids may be squeezed out resulting in islands of solid-solid contact, through which the contact stresses are transmitted. Water-filled channels surround islands of solid-solid contact, and are conduits through which material diffuses.

Microscopic observations demonstrate that the fluid topology in a low porosity monophase polycrystalline aggregate (as it is the case for crushed salt) is controlled by the balance between solid-solid and solid-fluid interfacial energies, and hence the dihedral angle θ (**Figure 2.7**). In the case of $\theta > 60^\circ$ the fluids will be present inside isolated inclusions, whereas for $\theta < 60^\circ$ the fluid forms an interconnected network of grain boundary triple junctions (Holness, 1997). In **Figure 2.7 a)** the geometry of the dihedral angle θ results from balancing of grain boundary interfacial energy (γ_{ss}) and solid-fluid interfacial energies (γ_{sf}); **Figure 2.7 b)** representation of idealized fluid distribution with cross-sections: the left grain shows a dihedral angle of $<60^\circ$ resulting in fluid distribution along a connected triple junction network; for $\theta > 60^\circ$ (right side) however, the fluid is restricted to isolated inclusions in triple junctions or along grain boundaries (Schenk, 2006).

Under relatively low stresses when dislocation creep mechanisms are slow, pressure solution creep (dissolution-precipitation or fluid-phase diffusional creep) is important. It is characterized by the dissolution of material at interfaces with a high differential stress, diffusion through a fluid phase provided by stress/strain induced gradients in solubility and precipitation at interfaces under low stress (e.g., Schutjens, 1991). Urai et al. (1986a,b) investigated fluid films by SEM

observations on deformed water-containing halite. Samples annealed for one year showed grain boundaries with isolated bubbles. The authors interpreted these results as evidence for the presence of brine films that shrink into isolated fluid inclusions after grain boundary migration stopped.

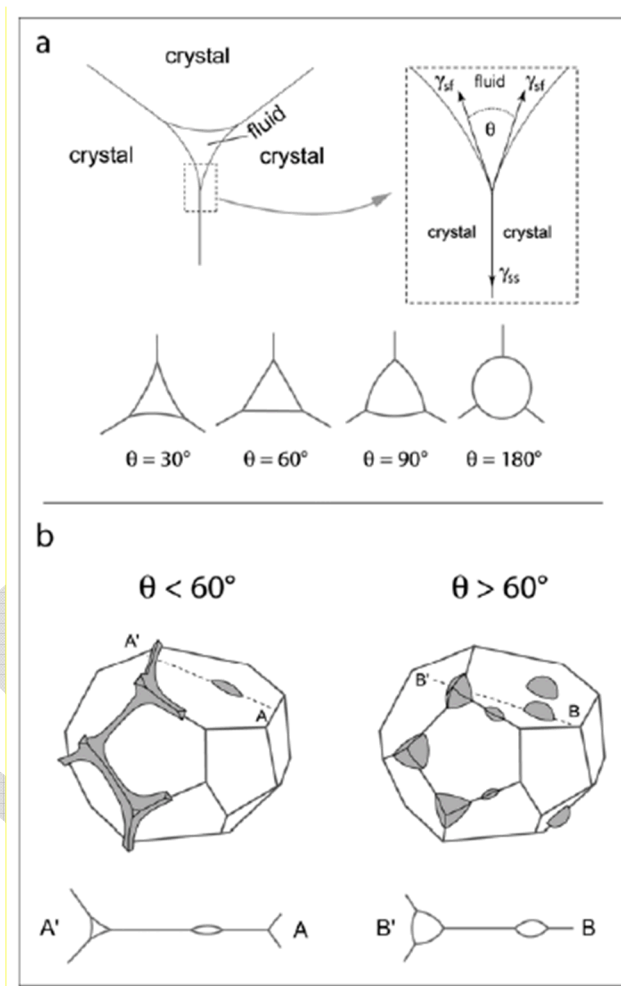


Figure 2.7 Schematic drawings showing the dihedral angle and its significance for connectivity of fluids in texturally equilibrated porous rocks.

The microscopic findings provide a consistent picture of fluid distribution and mobility inside granular aggregates as schematically shown in **Figure 2.8**. The nominal 35% void space is almost completely air-filled, which stands in stark contrast to the intact state of bedded salt: negligible moisture content (up to 1.0 wt. %) and negligible porosity. If granular salt is wetted to improve compaction and reconsolidation behaviour, the secondary moisture is mainly distributed at salt

grain surfaces as a thin wetting solution film or isolated as fluid droplets in grain interstices. Intracrystalline fluid inclusions captured during crystallization from the formation waters would remain inside the crystal structure, perhaps to be moved to the grain boundary by crystal plasticity. During isostatic compaction salt is transported by fluid-assisted diffusion processes, specifically dissolution and precipitation due to differences in chemical potential between points in the solid at grain boundaries under high stress and those under lower stress (**Figure 2.8**). As mentioned before, additional driving force (chemical potential drop) both along and across grain boundaries can be provided by internal plastic deformation of the grains, giving rise to combined grain boundary migration and solution-precipitation creep.

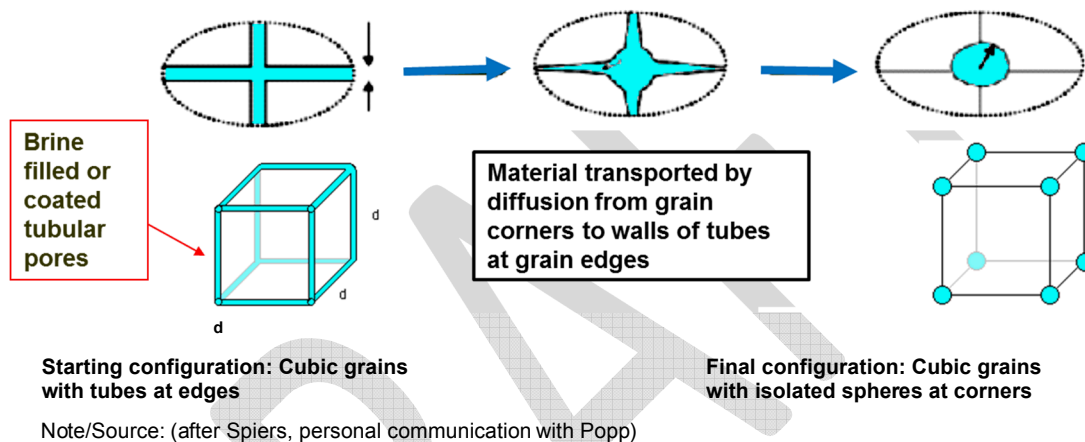


Figure 2.8 Schematic of fluid redistribution in granular aggregates during compaction.

The fluids existing in the primary pore space (mostly air and water vapor) are compressed and partially squeezed out during the transition to a low-pore-space regime. Migration out of the consolidating material continues as long as a connected porosity and adequate permeability exists. All observations confirm effective reconsolidation until only a few % porosity remains. At that point, the relative saturation within the intergranular pore space increases. As the granular salt continues to consolidate, further fluid transport out of the consolidating mass would undoubtedly involve two-phase flow of both brine and trapped air. Empirical results indicate that intrinsic medium permeability approaches zero as the porosity of the consolidating salt reduces. As this condition is approached the brine or air effective permeability are even lower than the intrinsic permeability and the mobility of fluids in highly compressed salt is very low. Of course, this range of conditions is very challenging to interrogate experimentally and remains an area of active research.

Residual gas contained in the pore space will be compressed within the fluid inclusions, developing a pore pressure. Some residual gas will also go into solution in the brine as pressure increases. If the pore structure were connected, the pore pressure may, in principle, counteract further compaction. The consequences of a local pore pressure on the overall compaction behavior and on fluid mobility have to be considered. As a first approach, basically the induced fluid-pressure impact is estimated to be low for a poroelastic effect because the pressurized area fraction in the grain structure is small. If a connected pore fluid pressure develops during reconsolidation, then the effective stress concept should be relevant. The effective stress (σ_{eff}) depends on the applied confining pressure (σ_m) and the pressure (p_{pore}) of fluid present in the pore space:

$$\sigma_{\text{eff}} = \sigma_m - p_{\text{pore}} = \sigma_m - \alpha \cdot p_{\text{fluid}}$$

The influence of the fluid pressure (p_{fluid}) is quantified by the Biot coefficient ($\alpha \leq 1$), which is not defined uniquely. For dilated intact rock salt, an empirical relationship between α and apparent sample permeability is presented in **Figure 2.9**, which contrasts strongly with granular salt. The data were derived from sophisticated short-term laboratory investigations of the dependence of gas permeability upon confining pressure and fluid pressure using pre-damaged salt samples (Kansy, 2007). Damage imparted to initially intact salt manifests parallel to the maximum principal stress. Fractures tend to propagate along grain boundaries, a small volume increase gives rise to a significant permeability increase because pathways are connected longitudinally. The McTigue (1986) point in **Figure 2.9** obtains when fluid pressure vanishes and the fluid is trapped locally in the pores.

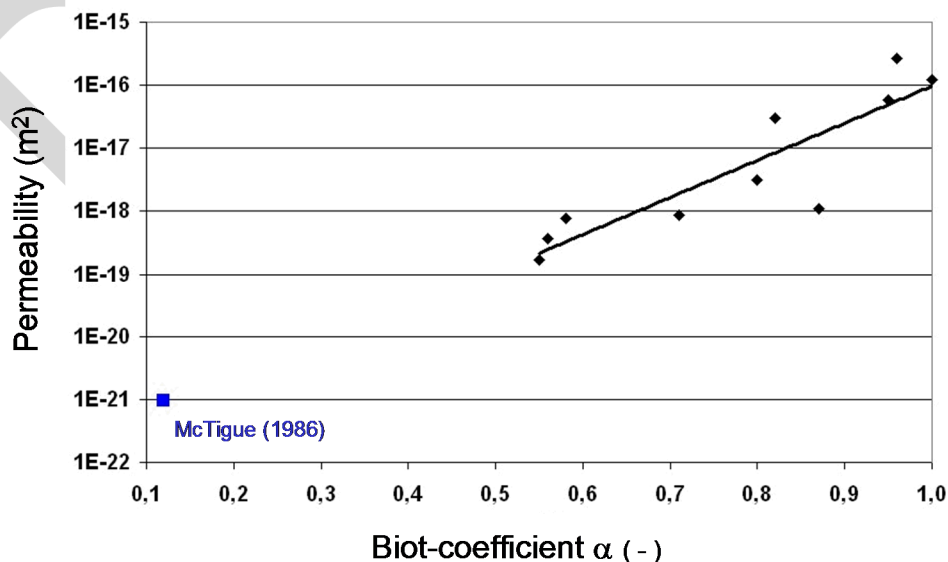


Figure 2.9 Relationship between gas permeability and the Biot-coefficient for dilated rock salt.

In Chapter 4 permeability data are given for consolidating granular salt using different fluids. Although estimated permeability depends strongly on the nature of the fluid used for measurements, the results clearly document permeability of the order $< 10^{-20} \text{ m}^2$ if the granular salt is compacted to porosity of a few percent. Thus, laboratory results confirm the influence of fluid pressure on effective stress becomes negligible (i.e., $\alpha \approx 0$) if the permeability is low; whereas, only under high porosity conditions, say granular salt with a porosity of $>10\%$ or in highly damaged salt is $\alpha \approx 1$, and p_{fluid} can bear some portion of the confining pressure, reducing effective stress. When α is low, fluid pressure does not reduce effective stress, and therefore brine doesn't reduce effective stress (i.e., the system approaches the well-drained limit of poroelastic behavior).

The assumption that pore pressures are of minor relevance to the final densification state is corroborated by microstructural observations. A grain texture with polygonal equidimensional mosaic texture is formed with 120° triple junctions owing mostly to pressure-solution at grain boundaries and suturing as redeposition occurs. In addition, distortion of individual grains via glide and climb mechanisms of dislocation creep allows grains to flow into and reduce void space. The remaining fluid is concentrated as fluid inclusions along grain boundaries or at grain corners. This evolution for granular salt consolidation is a close analogue to natural rock salt textures with isolated gas and brine inclusions at lithostatic pressure. Because there are no interconnections between occluded fluids they can no longer contribute to fluid transport, i.e., the effective porosity is zero.

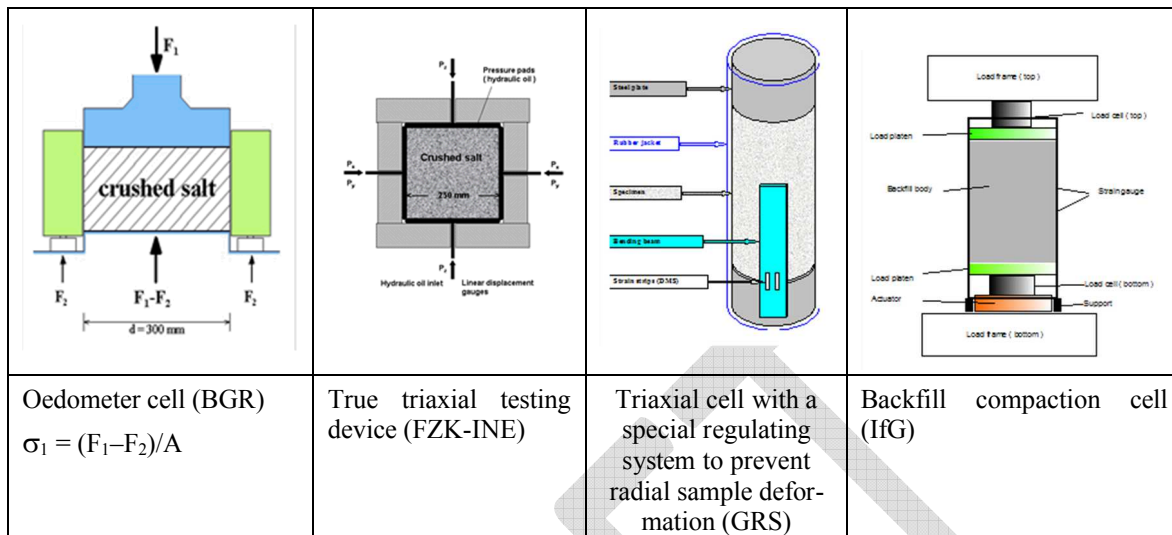
3 EXPERIMENTAL SALT RECONSOLIDATION MECHANICS

3.1 Experimental methodology

Laboratory experiments provide the opportunity to understand principal reconsolidation mechanics of crushed salt. Experimental laboratory investigations have been extensive. A recent, comprehensive review of the actual state of knowledge and accompanying data sets was put together within the framework of the German research project Restporosität und permeabilität von kompaktierendem Salzgrus-Versatz (Residual porosity and permeability of compacting granular salt backfill, REPOPERM) (Kröhn et al. 2009). Results showed sensitivity to lithological differences such as grain-scale variation, salt type, and humidity content. In addition, test results strongly depended on the variable conditions associated with test devices and test procedures. Thus, a reliable prognosis requires critical evaluation of the existing database for the various testing methods and procedures applied.

In the framework of the European Commission Project BAMBUS II (Backfilling and Sealing of Underground Repositories for Radioactive Waste in Salt) possible sources of error were systematically investigated by performing tests in different laboratories (BGR, FZK/INE, GRS, and IfG) using various state-of-the-art experimental setups. Figure 3.1 illustrates the testing techniques used for reconsolidation of crushed salt.

- an oedometer (BGR) - The dimensions of the cell determine the diameter of the sample for oedometer (for example, cell TRE-3002 has a diameter of 300 mm and a height around 150 mm)
- a true triaxial device (FZK-INE) - The measuring device has a cubic testing cell with a side length of 250 mm. The loading of the test material is independently controlled along the three spatial directions by using six hydraulic pressure pads (made of stainless-steel sheets) mounted at the walls of the cell
- an axisymmetric triaxial device (GRS) - The triaxial testing machine (von Kármán type) uses cylindrical samples with a diameter of 100 mm and 166 mm height. Lateral diameter measurement via strain gauges ensures a constant sample diameter during testing
- a backfill compaction cell (IfG) - In contrast to the usual oedometer cell, where the diameter-to-height ratio of the sample is about 2, the diameter/height-ratio in the compaction cell is 0.5. Accordingly, the samples used in the compaction cell are 310 mm high and 155 mm in diameter



Note/Source: (Bechthold et al. 2004)

Figure 3.1 Experimental reconsolidation set-ups.

In all tests operated by the various labs the relation between backfill pressure, (i.e., the mean value of the principal stresses) and porosity was determined. For a better comparison of the impact of different experimental setups, an assessment was made of the stress ratio $\lambda = \sigma_3 / \sigma_1$ for the oedometer-like test conditions. A common result noted in the tests was that the horizontal stress σ_3 generated in oedometer-like test conditions usually falls in the range between 30% and 55% of the vertical stress σ_1 . Another common observation was the trend for progressively increasing lateral stress with decreasing porosity and, thus, the resulting mean stress σ_m was determined to be a function of porosity.

Nevertheless, the experiments gave clear indications for methodical differences between the various test set-ups, mostly due to friction developed at the cell walls, which becomes part of the total load reflected by the pistons or loading plates. Therefore, experimental procedures need to be evaluated when applying results because the respective lab reconsolidation tests may be different. The most relevant uses of laboratory data are

- Estimation of the backfill pressure and porosity at the compaction rates in situ (e.g., $\dot{\epsilon} < 10^{-10} \text{ s}^{-1}$) if stabilization of underground openings is required
- Extrapolation to a residual porosity in the long term with respect to its sealing properties

Two principal investigation procedures are used to execute these types of tests, as illustrated in **Figure 3.2** (modified after Zhang et al. 1993). Type I shown in **Figure 3.2 a**) involves stress induced compaction using a constant deformation rate. Type II shown in **Figure 3.2 b**) involves

time-dependent compaction under constant stress conditions. Type I simulates converging underground openings with a constant displacement or loading rate. Due to the induced deformation, progressive hardening occurs until the stress approaches a practical limit, which corresponds to some residual porosity. The reliability of such tests may be limited due to time restrictions, i.e., within a reasonable period of time only limited compaction can be achieved. Experiments at BGR realized compaction rates and experimental conditions close to those in situ ($\dot{\epsilon} \leq 10^{-9} \text{ s}^{-1}$) by interpolating and extrapolating the curves of a σ_1/ϵ plot obtained at a number of different rates (**Figure 3.3**) Stepwise-increased compaction rates (from $\dot{\epsilon} = \sim 7 \cdot 10^{-10} \text{ s}^{-1}$ to $\dot{\epsilon} = \sim 7 \cdot 10^{-7} \text{ s}^{-1}$ using order of magnitude steps) have been used in the past. Type II experiments are constant-load creep tests that simulate time-dependent compaction processes, i.e., volume creep after pre-loading. Due to time-dependent relaxation processes (probably amplified by humidity-assisted weakening processes) a quasi-steady state compaction process is realized with decreasing rate according to the progressive porosity reduction.

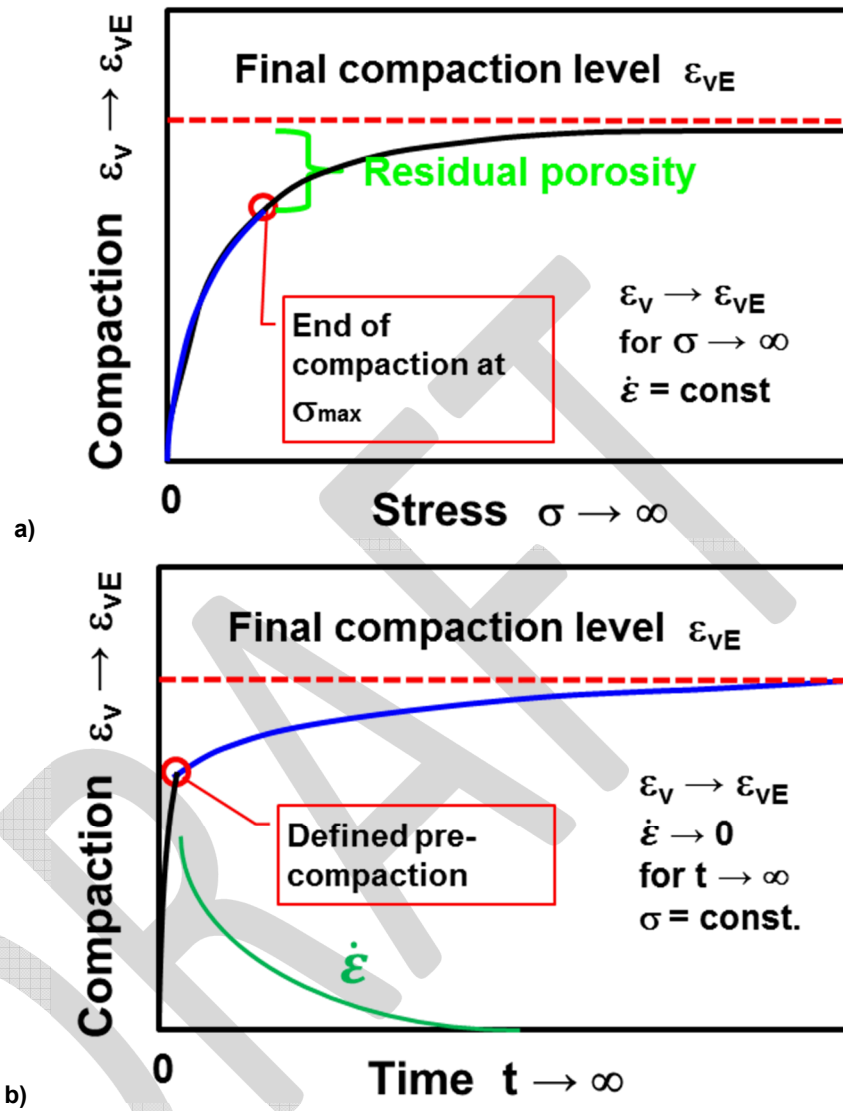


Figure 3.2 Compaction of crushed salt - schematics of experimental procedures.

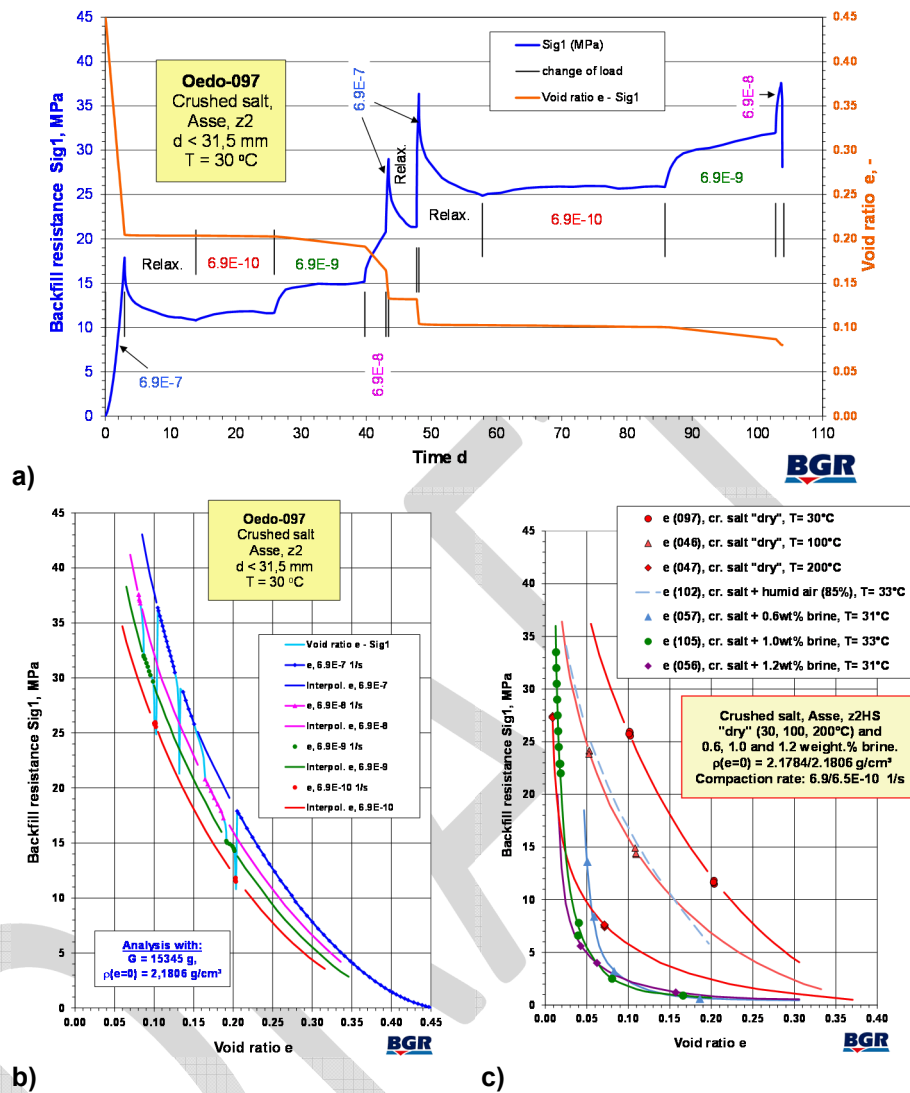


Figure 3.3 Consolidation behavior of granular backfill investigated under oedometer test conditions.

Much of the salt reconsolidation data base gained in the last three decades corresponds to experimental conditions of oedometer tests of the Type I description, which means that such types of experiments can be only interpreted regarding its final conditions using an appropriate constitutive law. In addition, during oedometer tests an increase of λ during relaxation phases was observed. This observation leads to the assumption that the stress ratio would increase if the tests had been extended over a still longer period of time, implying that under in situ conditions an approximation to unity (i.e., isotropic stress conditions) may be the natural condition.

3.1.1 Experimental results

3.1.1.1 Consolidation tests of Type I - strain-rate controlled loading

Results from BGR are given below for Asse salt backfill reconsolidation. The test depicted in **Figure 3.3 a)** and **Figure 3.3 b)** is a multi-step test of Type I with included relaxation phases and change of consolidation rate. This test was conducted on material possessing an initial void ratio of $e=0.45$ ($\Phi = 31\%$) at a constant temperature of 30°C temperature. Void ratio is the ratio between the pore volume (Φ) and the solid matter volume ($1-\Phi$) of the granular material. Void ratio and backfill resistance (σ_1) are plotted in **Figure 3.3 a)** for the test duration of over 100 days. Multiple consolidation rates were used as a means to facilitate a prognosis regarding porosity and load resistance at near in situ conditions of $\dot{\epsilon} \leq 10^{-9} \text{ s}^{-1}$.

Initially a relatively high constant displacement rate ($\dot{\epsilon} = 6.9 \cdot 10^{-7} \text{ s}^{-1}$) was selected to achieve a significant porosity reduction. Under these conditions, the axial load increased to around 18 MPa, while the void ratio reduced to 0.20. Then a relaxation phase was initiated, during which σ_1 decreased to about 11 MPa. After this significant stress drop occurred, stepwise-increased compaction rates were applied in decadal increments from $\dot{\epsilon} = 6.9 \cdot 10^{-10} \text{ s}^{-1}$ to $\dot{\epsilon} = 6.9 \cdot 10^{-7} \text{ s}^{-1}$. During each of the various steps a maximum loading stress level was reached, followed by a relaxation period and then continued at $\dot{\epsilon} = 6.9 \cdot 10^{-10} \text{ s}^{-1}$, which results in a near constant stress level at a specific void ratio. The interpolation lines in **Figure 3.3 b)** between the various measured stress levels at different void ratios represent the evolution of the backfill resistance at a given loading rate. The backfill pressure increases with decreasing void ratio, but it decreases with decreasing loading rate.

Furthermore, the backfill pressure strongly depends on the temperature and the moisture content. **Figure 3.3 c)** shows the backfill resistance versus void ratio as outcome from various tests with “dry” material at different temperatures (30° , 100° and 200°C) and wetted backfill at about 30°C (0.6, 1.0 and 1.2 wt.-% brine). The dashed line represents the results of a test with “dry” crushed salt, but charged with humid air at $T = 33^\circ\text{C}$. Only backfill stress levels corresponding to a proposed in situ rate of $\dot{\epsilon} = 6.9 \cdot 10^{-10} \text{ s}^{-1}$ are plotted in the diagram. It is evident that the resistance of crushed salt backfill is considerably smaller under high temperature or with small amounts of moisture. Under *dry* conditions and lower temperatures in such loading tests high stresses are required to reach final porosities of one or two percent corresponding to those of natural rock salt.

Under dry conditions high stress levels were required to achieve low porosity levels. An example of a high-pressure compaction test is given by Popp and Kern (1998). In this example granular salt sonic velocities approach those of natural, intact salt. In their experiments crushed salt with grain sizes around $200 \mu\text{m}$ were compressed at 120°C to stresses greater than 200 MPa.

Measurement of seismic wave velocities, V_p and V_s were used as an indication of complete compaction. During stress dependent reduction of porosities to nearly zero ($\sigma_{\text{hydr}} > 200$ MPa) they observed a nearly linear velocity increase for both V_p and V_s whereby the final values of $V_p = 4.56 \pm 0.1$ km/s and $V_s = 2.65 \pm 0.05$ km/s at maximum compaction correspond well to natural rock salt properties.

These results change significantly in the case of higher temperature or when small amounts of humidity are added to the granular salt. As can be seen from **Figure 3.3 c)**, under wet conditions the backfill resistance at a void ratio of 0.05 is on the order of 5 MPa as compared to 35 MPa for dry conditions. This observation supports the assumption that under natural wet salt conditions crushed salt will easily compact at stress levels well below lithostatic stress corresponding to repository depth. Nevertheless, investigations of Type I give no direct information about the time necessary to reach a final state where the consolidating granular salt achieves properties identical to the host salt. The results in **Figure 3.3 b)** lead to the assumption that the compaction rate of dry crushed salt drops considerably when the backfill resistance approaches host rock pressure. Hence, compaction rates in dry in situ conditions may become so small that a sufficient backfill compaction in a repository may not be reached within a reasonable time scale, such as the operational period or the period of institutional control.

3.1.1.2 Consolidation tests of Type II - creep tests

For an improved prediction of the temporal evolution of crushed salt under in situ stresses creep tests of the Type II are essential, i.e., monitoring of the decrease of granular salt porosity under a given confinement over time. Unfortunately, reliable long term measurements on natural backfill compaction are scarce. Representative test results for dry backfill, as well as for pre-compacted salt bricks are shown in **Figure 3.4**. **Figure 3.4 a)** is a BGR oedometer creep test in 1988/89 on dry crushed salt at a temperature of 100°C. The shown creep phase with an oedometer stress of 16.5 MPa (corrected for backfill resistance) resulted in a compaction rate of $\dot{\epsilon} = 1.4 \cdot 10^{-9} \text{ s}^{-1}$ after 75 days at a void ratio of 0.07 ($\Phi = 6.5\%$). After 150 days a rate of $\dot{\epsilon} = 7.2 \cdot 10^{-10} \text{ s}^{-1}$ was observed at a void ratio of 0.06 ($\Phi = 5.7\%$). The applied oedometer stress of 16.5 MPa is about 6 – 7 MPa ($\approx 30\%$) smaller than the result obtained in the strain controlled oedometer test 046 at $T = 100^\circ\text{C}$ plotted in **Figure 3.3 c)**. By comparison, a similar oedometer creep test from 1994/95 (not shown) with an applied oedometer stress of 14 MPa resulted after 60 days of compaction in a compaction rate of $\dot{\epsilon} = 8.3 \cdot 10^{-10} \text{ s}^{-1}$ at a void ratio of 0.1 ($\Phi = 9.1\%$). The stress of 14 MPa is only about 2 – 3 MPa (i.e., $\approx 10\%$) smaller than the expected result of test 046.

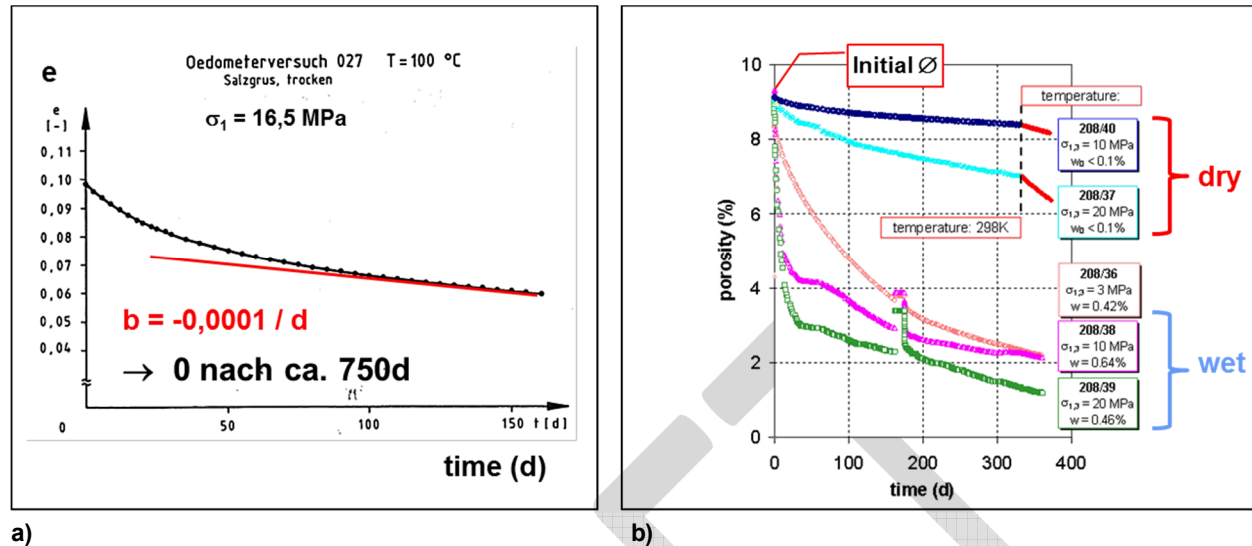


Figure 3.4 Consolidation tests of Type II – creep tests: a) oedometer test on dry crushed salt, b) isostatic creep consolidation tests on dry and wet salt bricks.

For a better understanding of humidity effects on the long-term properties, hydrostatic creep consolidation tests on granular salt were performed on artificial salt bricks (three wet and two dry) shown in **Figure 3.4 b)**. Tests were conducted for more than one year in special creep rigs (Salzer et al. 2007). In addition, in the dry experiments the temperature increased after 330d to 55 °C showing enhancement of the compaction creep. Comparing the various curves, as shown in **Figure 3.4 b)**, it can be clearly seen that notwithstanding the loading conditions, availability of small amounts of water is a controlling factor for reconsolidation.

Reconsolidation rates of the “dry” samples in **Figure 3.4 b)** are much slower than the moistened counterparts. If one extrapolates an approximation of the time-dependent compaction curves via a power function, the time required to reach a reference state of approximately 6% porosity would be around 8 – 9 years (for 20 MPa) and around 180 years (for 10 MPa). By contrast, the necessary time periods in moistened salt brick samples are only 9 days (for 20 MPa), 14 days at (for 10 MPa) and around 90 days at (for 3 MPa), illustrating rapid porosity reduction at low stress conditions.

Efficiency of reconsolidation changes with progressive densification. As shown in **Figure 3.4 b)**, initial compaction proceeds very fast on wet samples deformed at $\sigma_{\text{hyd}} = 10\text{ MPa}$ and 20 MPa . At around 50 days a remaining porosity of approximately 4% is reached and the reconsolidation rate slows appreciably. In contrast, the time dependence of the sample 208/36 ($\sigma_{\text{hyd}} = 3\text{ MPa}$) is

characterized by more gradual transient behavior until the final low porosity equal to tests at higher stress levels is achieved.

Additionally, variation of the temperature in the dry experiments from 25°C to 55°C allowed an estimate of the activation energy which was found to be in the order of $Q = 39$ kJ/mol (0.4 eV). Such activation energy is typical for material transport in rock salt by diffusion (e.g., Hunsche & Schulze 1990).

GRS is currently performing a set of long-term multistep creep tests in oedometers for qualification of constitutive models (Czaikowski et al. 2012). Three tests are in progress: one using a dried sample, a second with a sample of natural moisture content of about 0.1%, and a third artificially wetted one with a water content of 1%. **Figure 3.5** shows the porosity evolution of the three samples in response to axial stress steps noted in the legend in the upper right corner. Data are plotted to the end of calendar year 2013. The different deformation mechanisms discussed in **Figure 2.1** can be recognized in the mechanical response depicted in **Figure 3.5**. Every change in axial stress results in an instantaneous porosity reduction as a consequence of elastic and plastic deformation. At constant stress, viscous deformation can be observed. Deformation rates are considerably higher for the wetted sample in comparison to the other two, although axial stress is considerably less. The natural water content of the second sample (0.1%) is not sufficiently distributed to promote humidity-induced processes.

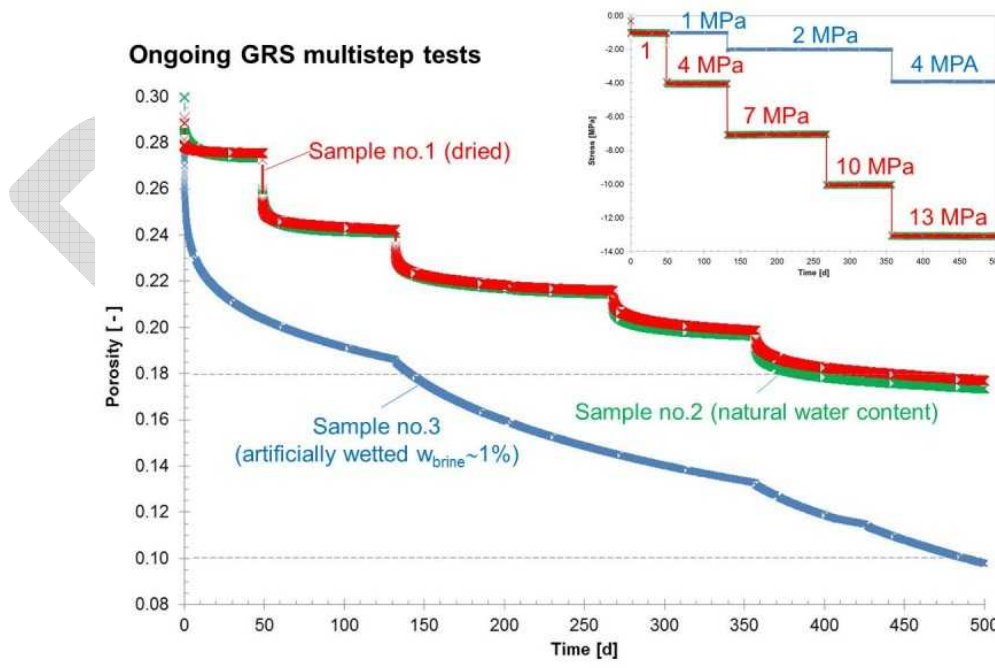


Figure 3.5 Ongoing multistep oedometer tests at GRS.

BGR has previously conducted several triaxial compaction tests in a von Kármán cell on pre-compacted “dry” crushed salt (Bechthold, 2004). The spatial stress state is determined by the load components and can be used to assess validity of constitutive equations. The compaction of the sample is found by measuring the reduction of the air filled pore volume using a special burette. However, the accuracy of the results has not been satisfactory enough due to scatter in the creep compaction results.

An improved volume measurement has been used in the triaxial compaction creep test TK-031, which is plotted in **Figure 3.6**. A uniaxial precompacted sample has been consolidated with the different isotropic stresses $\sigma = 10, 12, 15, 18$ and 20 MPa from $e = 0.197$ to $e = 0.074$ ($16.5\% > \Phi > 6.8\%$) in about 300 days. **Figure 3.6** shows the volumetric strain rates versus void ratio, the volumetric strain versus time (2nd axis) and some manual extrapolations of the curves which may represent the possible material behaviour down to porosities approaching that of the host salt. Unfortunately the sample had to be unloaded several times due to power outages. With a best-fit curve in a σ - t plot the volumetric strain rates have been analyzed for every section with constant load.

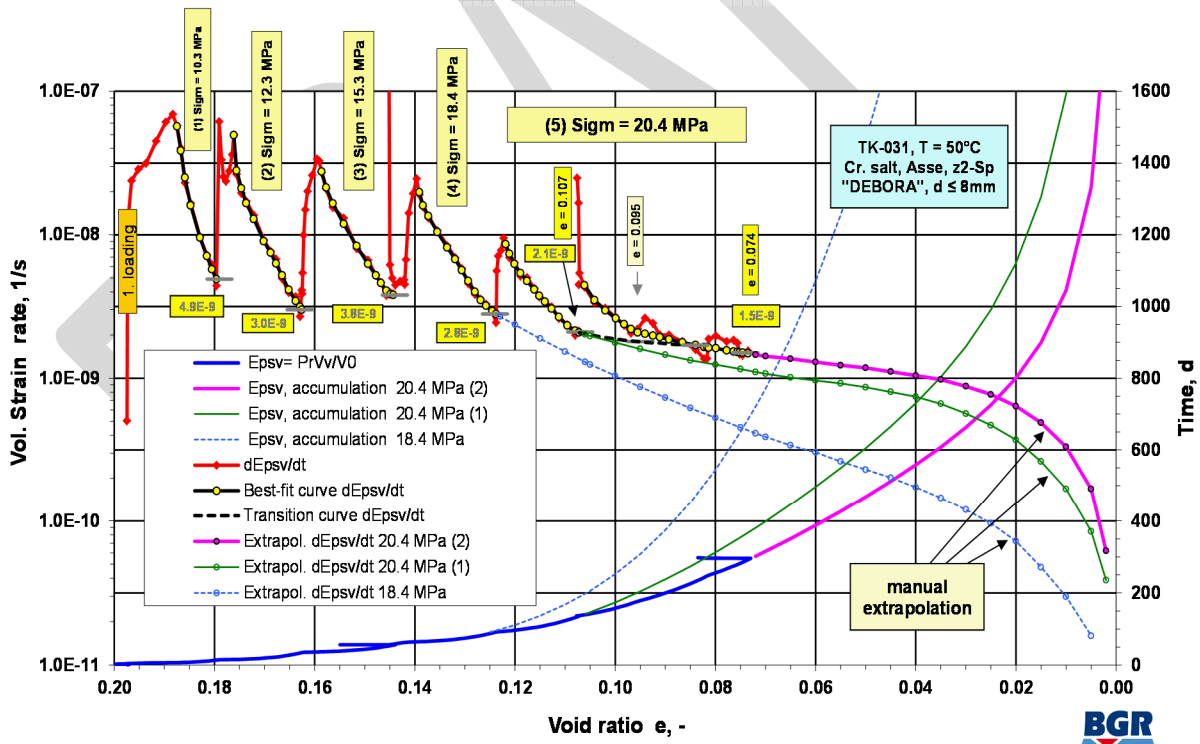


Figure 3.6 Triaxial compaction test TK-031.

Characteristic data illustrating the relation of the compaction rate to the applied stress and the current void ratio have been selected at a time when the influence from the last load increase phase on the compaction rate has apparently decayed. The last load phase lasting over 200 days applied an assumed host rock pressure of $\sigma \approx 20$ MPa; this provides results in the stage of lower porosities. In all compaction phases the volumetric strain rate did not fall below 10^{-9} s^{-1} . The extrapolation of the strain rate curves is estimated, without application of an explicit mathematical model. The strain rate will decrease progressively due to advanced compaction as illustrated by the three different examples in the diagram:

The magenta curve shows the extrapolation of the test stage with $\sigma_m = 20.4$ MPa based on results at the end of the test. The green extrapolation is also based on the $\sigma_m = 20.4$ MPa stage, but follows the trend of the strain rate observed before reloading at $e = 0.107$. The blue curve extrapolates the test stage with $\sigma_m = 18.4$ MPa. The strain curves were calculated by summation using increments of $\Delta e \leq 0.005$. The entire compaction time required to achieve a void ratio of $e = 0.02$ ($\Phi = 2.0\%$) is about 800 days (2.2 years), 3 or 11 years in the case of the magenta, green or blue curve, respectively. To attain a void ratio of $e = 0.002$ ($\Phi = 0.2\%$), a compaction time of 5, 8 or 34 years would be required according to these estimates.

In **Figure 3.7** the results of test TK-031 are compared with the data of the strain controlled oedometer test 049 in a plot of mean stress versus void ratio (σ_m - e -plot). The isolines generated for constant compaction rates spaced at one order of magnitude are used to assess the trend of the volumetric strain rates of TK-031. At the calculated mean stress σ_m of oedo-049 the smaller lateral stress component in the test structure is taken into account. A formula developed by Korthaus in the BAMBUS II report of Bechthold et al. (1999) was used although it is not validated at lower porosities.

In the constant compaction phase with $\sigma_m = 20.4$ MPa of TK-031, in which the void ratio was reduced from 0.107 to 0.074 in about 160 days, the volumetric strain rate exhibited only minor decrease from $2.1 \cdot 10^{-9}$ to $1.5 \cdot 10^{-9} \text{ sec}^{-1}$. The isolines of the oedometer test, however, suggest a decrease of about three orders of magnitude. Hence, the postulated precipitous decrease of the compaction rate has not been confirmed by test TK-031.

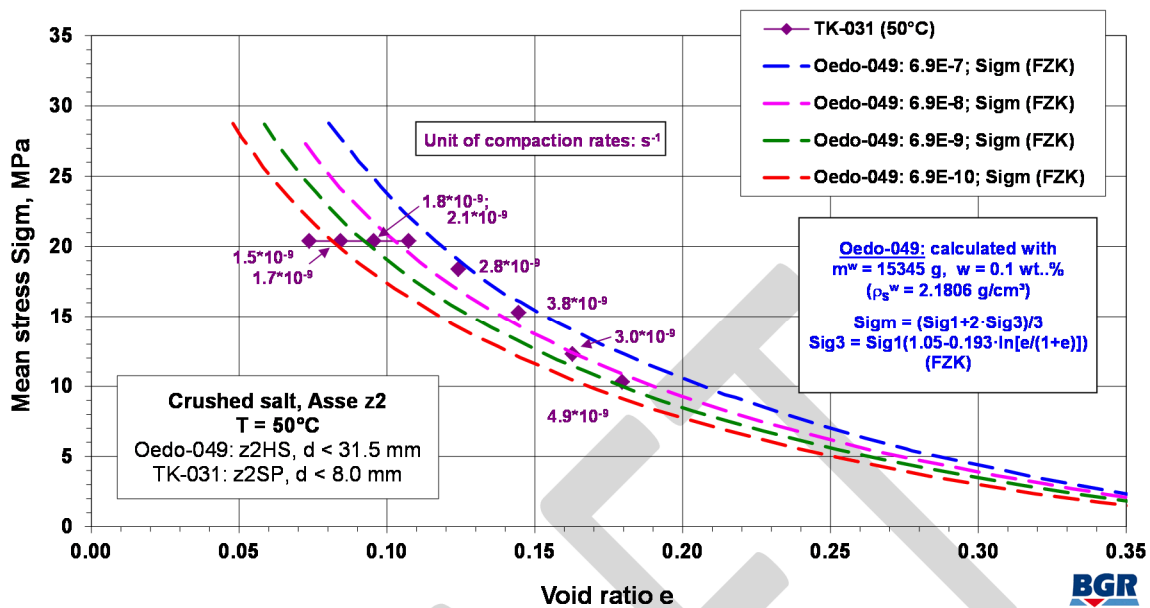


Figure 3.7 Comparison of volumetric strain rates at 50°C . Triaxial compaction test TK-031 and oedometer test Oedo-049.

Summarizing these examples of existing data, it becomes clear that the acting processes under a variety of experimental conditions are well understood and reliable. The principles of consolidation are understood well enough that extrapolation to large-scale field applications seems feasible. Further, as pointed out here, testing techniques can influence consolidation processes and it is therefore imperative to understand these fundamental physical phenomena when applied to repository seal systems. In that regard, we strongly recommend reliance on experiments of Type II. Triaxial tests should be given preference, as isotropic test conditions are more representative of in situ conditions than oedometer tests.

3.1.2 Improvement of the compaction behavior – role of additives

The previous chapters demonstrate that existing knowledge provides confidence that crushed salt will compact at relatively low lithostatic stress conditions to a negligible porosity within a limited time. Application of straightforward construction techniques should readily affect high performance seals within the nominal operational period of nuclear waste repository. Further, granular salt reconsolidation can be easily modified with small additions of moisture to take advantage of the improved reconsolidation process promoted by water films. Other relatively simple considerations such as mixing to reach a final grain distribution close to the Fuller curve (ideal gradation) can improve reconsolidation in situ (M. Gruner, personal communication). In general, elevating the temperature of salt aggregate accelerates reconsolidation. If we desire to

guarantee high performance in the very short term, clay additive may prove an alternative that can achieve performance specifications upon construction.

Recent research sponsored within the European Union research project NF-PRO (Stührenberg, 2004; 2007) focused on laboratory testing mixtures of crushed salt and bentonite for conventional shaft sealing purposes. The addition of Ca-bentonite and natural clay can reduce permeability of the backfill considerably at room temperature. Examples of the effective reconsolidation enabled by adding Ca-bentonite to crushed salt (with or without added brine) are shown in **Figure 3.8**. Tests were conducted at the BGR (Stührenberg, 2007) using an oedometer arrangement and applying a consolidation rate of $6.9 \cdot 10^{-10} \text{ s}^{-1}$. **Figure 3.8 a)** plots backfill stress versus void ratio for several mixture ratios. The curve for pure crushed salt is plotted for comparison. Results clearly document the favourable effects of additives. At a void ratio of $e = 0.1$, for example, the pure crushed salt backfill resistance is more than 25 MPa. With an addition of 10 to 20% Ca-bentonite the backfill resistance can be reduced to values between 6 and 8 MPa. A further decrease to less than 4 MPa is attained with a small amount of brine in the sample. An 85% salt/15% bentonite mixture shows the smallest backfill resistance in comparison to those without added brine until a void ratio of $e \approx 0.05$ is achieved. **Figure 3.8 b)** shows little effect of elevated temperature on reconsolidation tests of 85% salt/15% bentonite mixture. Further reconsolidation tests (e.g., performed by IfG, 2012) confirmed this effect showing similar backfill resistance values for the respective mixture.

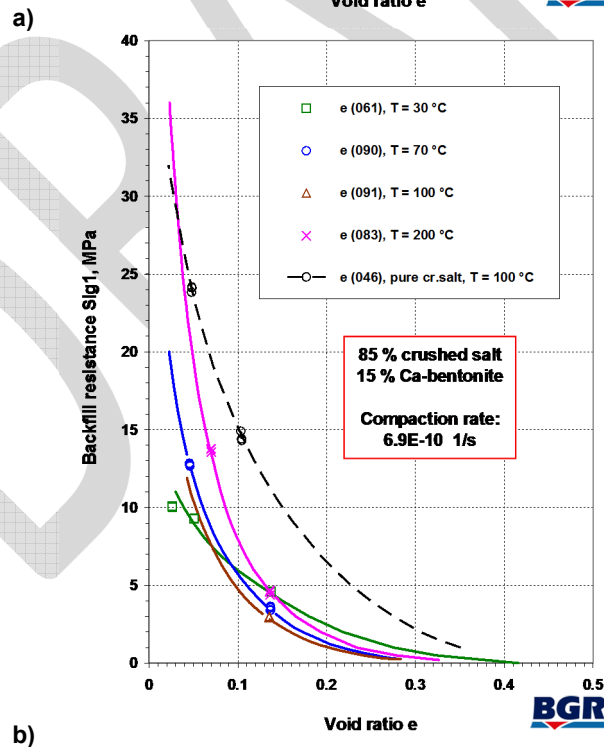
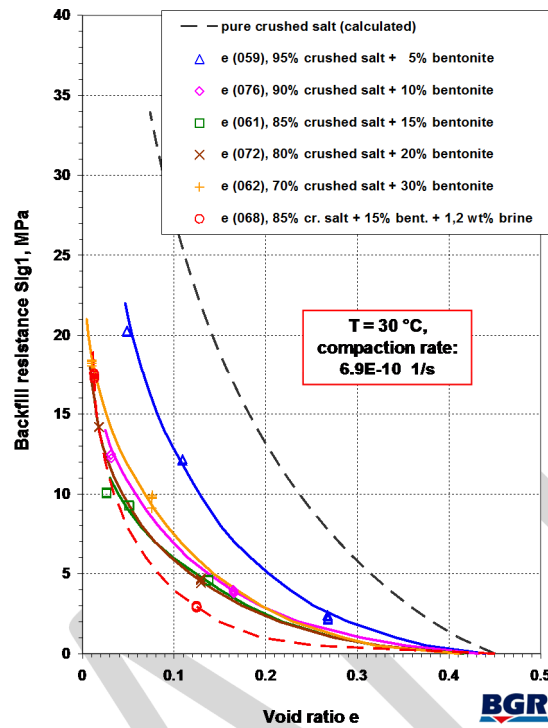


Figure 3.8 Impact of additives on the compaction behavior of crushed salt.

Addition of clay, commonly bentonite, obviously improves porosity reduction behavior of salt aggregates. The fundamental processes and the underlying microstructural interactions have not been well investigated to date. As a preliminary hypothesis, the clay particles likely reduce friction along grain boundaries. From a mechanistic point of view, the findings of Renard et al. (2001) are intriguing. They suggest clay particles trapped along salt grain contacts enhance pressure solution by sustaining open grain contacts. This microstructural arrangement would favor diffuse transport of Na^+ and Cl^- to the pore space and inhibit grain boundary formation. At higher temperatures, as shown by the results in **Figure 3.8 b**), the effect of backfill resistance reduction seems to be progressively reduced. As a possible explanation the moisture content of the bentonite may be reduced due to some drying, which would be expected to influence the compaction behavior. Additional studies of the underlying microstructural and physical-chemical processes will help clarify these phenomena.

4 TRANSPORT PROPERTIES OF COMPACTED CRUSHED SALT

4.1 Methodology

Permeability is usually determined in a combined compaction-permeability tests using a triaxial setup with axial flow geometry. The porous sample is compacted stepwise by application of isostatic pressures, i.e., the axial σ_1 and the confining pressure σ_3 are equal. At constant loading conditions the fluid flow q is measured through a sample with defined geometry for a given pressure gradient, generally. For linear flow of an incompressible fluid of viscosity η (usually oil or brine) the fluid permeability can be derived from Darcy's equation:

$$k = \frac{\eta_{\text{brine}} \cdot q \cdot l}{\Delta p \cdot A}$$

with k = permeability (m^2) A = sample cross section of the sample (m^2)
 l = sample length (m) η_{brine} = dynamic viscosity ($\text{Pa} \cdot \text{s}$)
 q = volumetric flow rate (m^3/s) Δp = hydraulic gradient (Pa)

For compressible fluids, i.e., gases, a modified form has to be used whereby the viscosity of gases η_{Gas} (e.g., air) is a factor of 60 lower than for water:

$$k = \frac{2\eta_{\text{Gas}} \cdot l}{A} \cdot \frac{q \cdot p_L}{(p_1^2 - p_2^2)} \quad \text{with } P_1 = \text{injection pressure and } P_2 = \text{outlet pressure}$$

Prerequisites for the determination of reliable transport parameters are:

- laminar flow
- steady-state flow (no fluid accumulation in sample)
- no reaction between the measuring fluid and grain boundaries
- single-phase flow

4.2 Permeability/porosity relationships – natural rock salt vs. compacted crushed salt

Time dependent deformation of crushed salt as well as intact salt rocks under various stresses results in a change in the transport properties described primarily by porosity and permeability. The physical processes are substantially different, which gives rise to very different permeability/porosity relationships. Intact salt possesses unmeasurably low permeability (Beauheim and Roberts, 2002). Referring to **Figure 4.1**, as intact salt is deformed under dilating conditions, the originally nearly impervious ($k \ll 10^{-20} \text{ m}^2$) material develops a rapid increase in permeability up to 10^{-15} m^2 depending on pressure despite very small increases in porosity

(<0.5%). Typically in dilating laboratory conditions, porosity is reflected by volumetric strain measurements, which have been directly correlated to damage. Consolidation of crushed salt (initial porosities 30 – 40%) yields a vastly different trend in the opposite direction with a clear decrease of the permeability to $<10^{-18} \text{ m}^2$ for porosities on the order of 10%. Thus, a unique (i.e., non-hysteretic) permeability/porosity relationship for the material “salt” does not exist.

Two very different phenomena and underlying deformation mechanisms are at play. Intact salt exhibits damage by grain boundary separation parallel to the maximum principal stress. Fractures tend to propagate and grow such that the vast majority of the volumetric strain is contributed by a few longitudinal pathways, which are conducive to advective flow. Granular salt, by contrast, acts as a porous medium until connectivity of pores is eliminated by suturing of grain boundaries. From the empirical evidence, grain-to-grain healing begins to inhibit flow while appreciable void space remains in the material.

For intact rock salt various authors (e.g., Stormont and Daemen, 1992; Peach and Spiers, 1996; Popp et al. 2001) have shown that microcrack dynamics control the permeability evolution during triaxial deformation of dry rock salt samples resulting in a rapid increase up to several orders. In a first approximation the relationship between permeability k and porosity Φ can be described by the simple approach

$$k = \Phi^n$$

From **Figure 4.1** it can be seen that the permeability/porosity data for dilatancy in rock salt have to be fitted by a two-regime model if a parabolic relationship is assumed. The initial opening of pore space corresponds to an exponent $n \sim 2-4$. As damage accumulates the increase of permeability is only weak or constant ($n \approx 0.2 - 0.4$). In the more damaged regime the order of permeability has also been shown to be a function of the minimal pressure (Popp, 2002).

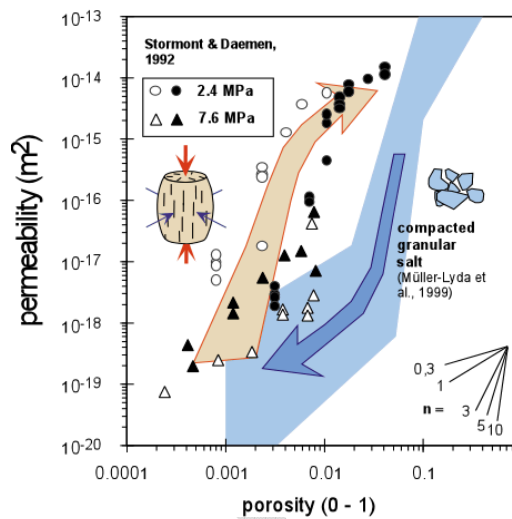


Figure 4.1 Permeability-positivity relations of dilating rock salt and reconsolidating granular salt.

Granular salt reconsolidation proceeds by closure of porosity enhanced by dissolution-precipitation processes, which strongly modify the geometry of the pores resulting in a rapid decrease of permeability. A comprehensive evaluation of results of several working-groups on the permeability-positivity relationship for crushed salt at different compaction levels is given by Müller-Lyda et al. (1999). Their analysis indicates an enormous scatter of the permeability data depending on lithological parameters such as grain size distribution, experimental conditions (triaxial versus oedometric tests) and moisture content. Reconsolidation of crushed salt with initial porosities between 30 – 40% results in sharp decreases of both porosity and permeability corresponding to an exponent n between 5 and 10.

It follows that a permeability/positivity relationship during dilatant deformation of salt and the reverse process of consolidating salt cannot be described by only a single-valued function. The transformation of the characteristics of highly compacted crushed salt to those of natural rock salt is fundamentally different at the microscale. At the same time, it becomes obvious that reconsolidation of granular salt efficiently restores the hydraulic integrity of the former crushed salt. Significant data scatter attendant to these types of experimental measurements necessitates sophisticated evaluation when discerning realistic permeability ranges corresponding to the material state.

4.3 Impact of two-phase flow phenomena

Although some details regarding two-phase flow in salt at low moisture content are poorly characterized, it is clear the relative permeability of salt to brine and air are both lower than the

intrinsic permeability. Traditionally two-phase immiscible flow involves wetting (brine) and non-wetting (gas) fluids which do not interact with the solid phase. Especially at low brine saturation and high confining pressure, the fluid is interacting with the salt through fluid-assisted deformation mechanisms. Two-phase flow requires relative saturation of each phase be related to pressure through empirical moisture retention functions. Relative permeability, a function of pressure, is given by related empirical functions either experimentally determined or derived from the moisture-retention functions analytically. Few laboratory data exist to constrain these two required relationships for intact salt or reconsolidating crushed salt. The low intrinsic permeability of salt makes the laboratory tests required to characterize these functional forms difficult and time consuming. Although there are more data available for clays, the two-phase flow model does not strictly apply to swelling, creeping, and compacting clay-rich rock either, but it has been widely applied there due to the lack of well-established more appropriate models. Although some of the fundamental assumptions related to two-phase flow in salt, such as noninteracting fluid, are violated, we can still qualitatively infer permeability to brine and gas will be lower than the intrinsic permeability of the medium.

Laboratory data at very low brine saturation under different compaction and stress states may allow more accurate simulation of two-phase flow in reconsolidating salt. Moisture retention function data are available for granular salt which is not fully compacted (e.g., Cinar et al. 2006 and Olivella et al. 2011). We do not have enough experience or low-porosity data to use the two-phase flow model as proof for immobility of fluids in fully compacted crushed salt.

Voids within the consolidating granular salt contain both air and brine, some of which will remain as the porosity becomes very small. This residual fluid may not have pathways available to escape during progressive compaction. As the air and brine are squeezed into the remaining porosity fluid transport may occur as two-phase flow and/or a local pore pressure may be generated.

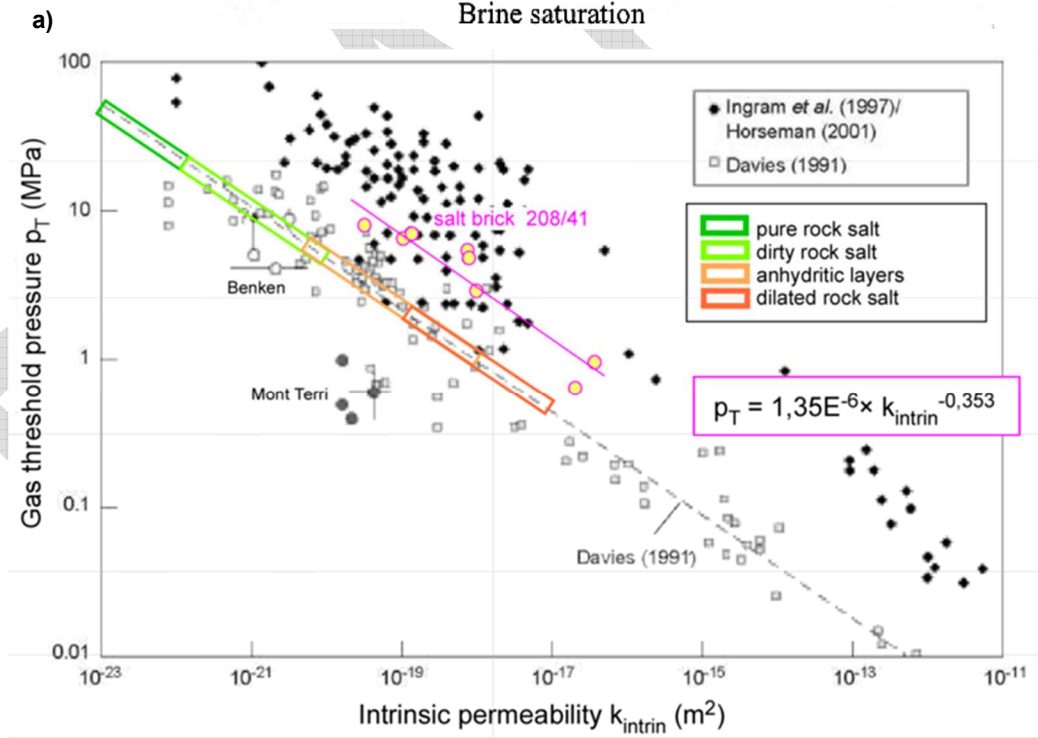
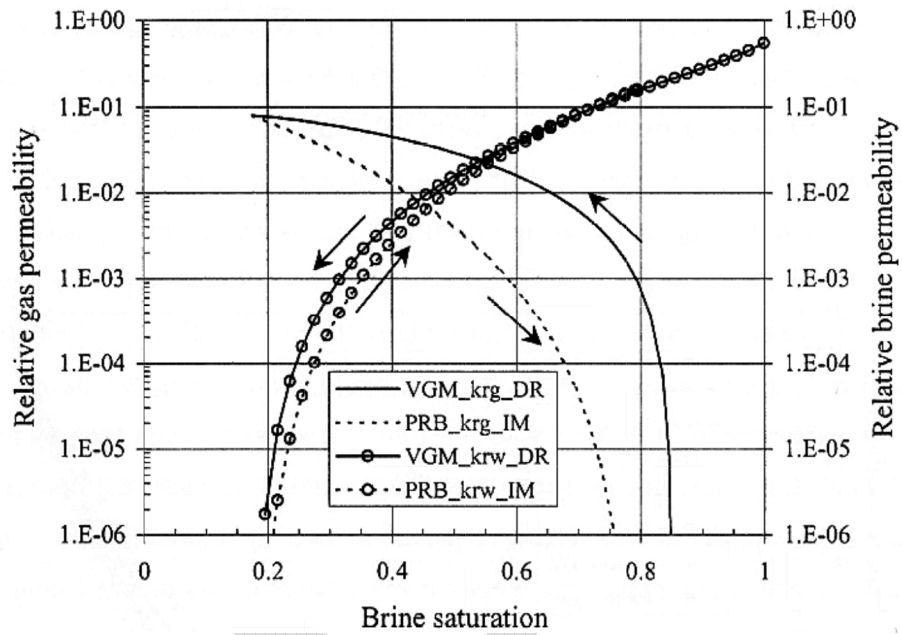
Whereas the later pore pressure effect has been found to be of minor importance for the overall compaction behavior, the fluid mobility and possible transport properties are significantly affected by two-phase flow phenomena as shown in **Figure 4.2**

- The resulting effective permeabilities at significant levels of brine saturation in the pore space (0.2 - 0.8) are up to several orders of magnitude lower than the salt matrix intrinsic permeability (**Figure 4.2 a**). These effective permeabilities are predicted by models developed for non-salt porous media (i.e., sands). Despite this lack of data, salt and brine would be expected to qualitatively follow similar trends, although the functional form may be quite different at low brine saturation. Heterogeneity can often

be a more significant source of uncertainty than the exact functional form of moisture retention and relative permeability distributions for a given set of fluids and porous medium.

- Due to the occurrence of capillary threshold pressures, very high fluid pressures are required for alternating displacement of gas and brine, depending on the opening width of the present pore-space pathways. This becomes obvious from the relationship between capillary gas threshold pressure vs. intrinsic permeability for different salt types as shown in **Figure 4.2 b**), mainly derived from empirical relationships for a wide variety of geologic materials (core measurements) and estimated threshold pressure ranges for various lithologic units in the Salado Formation (after Davies, 1991). In addition, results of gas breakthrough measurements on compacted salt bricks (lab no. 208/41) are given (Salzer et al. 2007). If permeabilities are $\leq 10^{-18} \text{ m}^2$, fluid pressures on the order of several MPa are required to mobilize fluids in the salt matrix.

Some portion of the initially free intergranular brine will ultimately become isolated brine inclusions on the boundary between salt grains and brine content in non-salt (anhydrite or clay) layers. The remaining brine will saturate the salt's intergranular porosity, which has been estimated from hydrostatically loaded salt cores to be 0.1—0.2 volume percent (Stormont and Daemen, 1992). Despite the increasing saturation accompanied with a local pore pressure in the final stages of crushed salt-compaction (relative permeability is increasing), intrinsic permeabilities are decreasing and connected pathways which may allow fluids to escape are being eliminated. Based upon data for intact salt, we know the brine permeability of salt away from the excavation disturbed zone is essentially unmeasurable (Beauheim and Roberts, 2002). Pore pressure in intact salt away from the excavation disturbed zone, when measurable, is approximately lithostatic. Observed brine permeability and pore pressure away from the disturbed zone indicates there is no local pore-pressure gradient to drive flow and no permeability to conduct the brine. It has been shown that reconsolidated crushed salt will eventually become like intact salt. The impermeable nature of intact salt is one of the primary benefits of using salt a repository host rock.

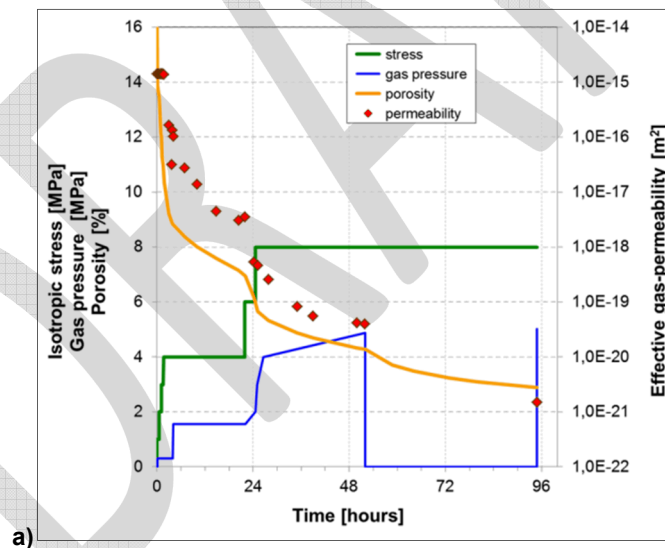


a) Relative permeability functions predicted by various models (Cinar, 2000). b) Plot of gas threshold pressure vs. intrinsic permeability.

4.4 Results from laboratory testing with a crushed salt / clay mixture

According to the methodology described previously, the permeability of salt/clay mixtures are determined stepwise during isostatic loading. The porosity is determined either from the subsequent measurement of the specimen dimensions (after unloading from a specific test stage) or directly derived from the continuously measured volumetric deformation of the specimen.

Typical results are presented in **Figure 4.3**. In both tests the general loading conditions and fluid pressures are given (IfG, 2012). Permeability is measured during loading tests on clay/crushed salt mixtures wetted with approximately 4.5 wt. % brine. Such a material might be appropriate for a long-term shaft seal in a salt formation. During both tests (one of them a short-term test of 4 days duration with gas injection and the other a long term test of more than 60 days duration with brine injection) the confinement ($\sigma_{ax} = \sigma_3 = \sigma_{iso}$) was increased stepwise with simultaneous fluid injection (gas or brine, respectively) at constant fluid pressure and measuring the constant flow rate. The clay/salt mixture was pre-compacted simulating field construction and stress history during and after plug installation in the shaft. Initial porosity is around 15% corresponding to permeability of the order of 10^{-16} m^2 .



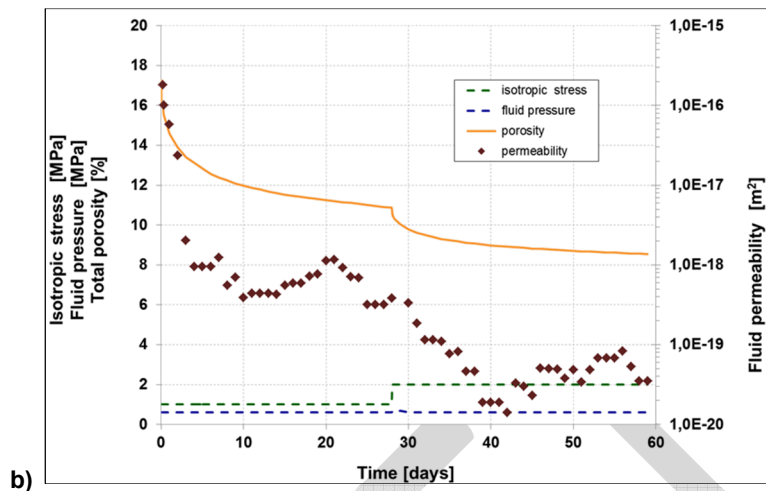


Figure 4.3 Transport properties of crushed salt/clay aggregates using gas a) and brine b) .

Both diagrams show increase of confinement results in a significant decrease of porosity and permeability. Under wet conditions the permeability drop is more pronounced than for the nominal “dry” case. (See **Figure 4.3 b**.) Both tests demonstrate that at static stress conditions reconsolidation proceeds with associated permeability decrease. In the short term test at a final confinement of 8 MPa the measured final porosity is in the order $3\% \pm 1\%$ and the measured gas-permeability is $< 10^{-20} \text{ m}^2$. Fluid droplets were observed at the end-pistons after the experiment. Presence of fluid indicates late-stage squeeze-out of some fluid amount from the pore-space, which would be at least partly saturated. Thus, two-phase flow phenomena may affect the results when permeabilities become very low (10^{-20} m^2). In the longer-term test plotted in **Figure 4.3 b**) a pure brine-permeability (saturated state) is measured. At a modest hydrostatic pressure of 2 MPa and a residual porosity of around 8% a low brine permeability in the order of 10^{-20} m^2 was determined, which corresponds to the measuring resolution of the equipment and confirms attainment of very favorable sealing properties.

4.5 Transport properties of compacted crushed salt - synthesis

The systematic study of transport properties of crushed salt has included extensive work by different research groups, which applied a variety of experimental approaches and setups. Key studies of WIPP salt are Brodsky (1994), Brodsky et al. (1996), Hansen & Ahrens (1996), and Case et al. (1987). Relevant German studies are reviewed in the framework of the REPOPERM project (Kröhn et al. 2009), which also considers the datasets already represented in Müller-Lyda et al. (1999). **Figure 4.4** is a synoptic diagram of these myriad results.

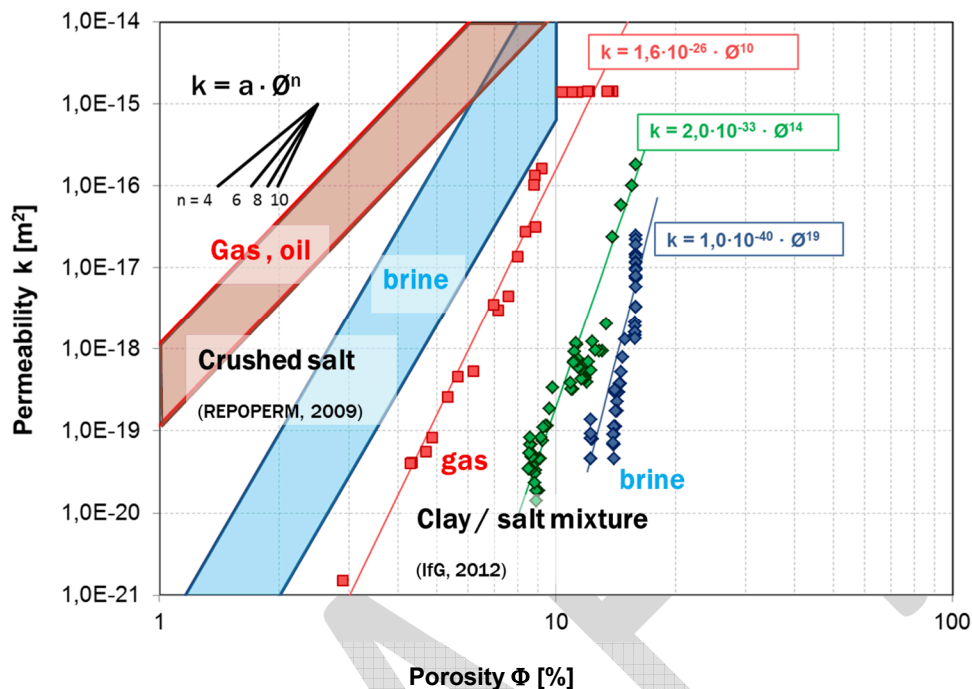


Figure 4.4 Synoptic view of permeability-positivity data sets for crushed salt aggregates.

In evaluating the various sources of permeability data for crushed salt, as depicted in **Figure 4.4**, the following conditions have to be considered:

- *Porosity* (respectively fractional density): the porosity of crushed salt ranges from around 40% (crushed salt debris) over a specific porosity (depending on pre-compaction) to a negligible porosity comparable to undisturbed rock salt, say 1-2%. Accordingly, the magnitude of permeability varies over several orders. The main focus of our study is the porosity range <20%, because performance measures of interest are attained at low porosity. Once again we note that permeability results from interconnected pore space and its shape, which is described as *effective porosity* which is smaller than the overall determined porosity.
- Crushed salt lithology:
 - Grain size distribution: the influence of grain size distribution may be relevant at higher porosities because the finer particles fill the voids between the larger grains. However, construction techniques that apply dynamic compaction or other densification measures will greatly modify particle size and distribution.

- Mineral composition (i.e., origin) of the crushed salt: the amount and distribution of impurities controls the inter- and intra-crystalline deformation processes of the main constituent rock salt. For example, coarse grained anhydrite aggregates along grain boundaries may hamper closure of grain boundaries and cracks and inhibit healing.
- Fluid content:
 - Water may enhance local deformation processes at grain contacts, which interrupt fluid pathways.
 - Water films along grain boundaries may induce 2-phase flow processes and capillary threshold effects, thus lowering the effective permeability.

In addition, because physico-chemical interactions may also be of importance; the *nature of the fluid* used for permeability measurements has to be taken into account. The results documented in REPOPERM (Kröhn et al. 2009) represent measurements which were determined using the following fluid media:

- oil - due to the use of a nonpolar liquid hydro-chemical interactions between the measuring fluid and the crushed salt are excluded but humidity-induced deformation processes at grain boundaries are hampered.
- gas - in the laboratory nitrogen is generally used as inert gas of high quality, (i.e., dry gas) which means that drying of a natural wet salt sample cannot be excluded.
- brine – saturated salt solutions, which are chemically equilibrated against the salt matrix. However, due to physico-chemical interactions (solution/precipitation) at typical stress and temperature gradients within a loaded sample the measurements of brine flow during loading at increased temperatures is extremely challenging. Although temperature effects have limited application in salt repository seals, there are a few reliable results available, mostly from the BGR and the Working Group Darmstadt (Elliger, 2004).

Figure 4.4 summarizes various permeability data sets which were identified as reliable and comparable for crushed salt, measured with gas and brine and depicted as two variation fields. Also plotted are individual measurements of 3 test series on clay/salt mixtures measured with gas and brine, respectively. The relevant porosity ranges from around 20% to 1%, i.e., the backfill material represents compaction levels as might be applied in salt repositories. Despite the data scatter for salt/clay mixture and somewhat broad bands indicated for crushed salt, it becomes obvious that

- independent of the material (crushed salt or clay-salt mixtures) the permeability-porosity relationship under wetted conditions lies always below the field determined with non-polar fluids or nominal “dry” conditions, i.e., for the same porosity the corresponding permeability is several orders lower for wet conditions (brine) than for dry conditions (oil or gas).

For example at $\Phi = 2\%$ $\Rightarrow k_{\text{crushed salt-dry}} \approx 5 \cdot 10^{-18} \text{ m}^2$ to $5 \cdot 10^{-17} \text{ m}^2$; $n \approx 5$

$\Rightarrow k_{\text{crushed salt-wet}} \approx 1 \cdot 10^{-21} \text{ m}^2$ to $1 \cdot 10^{-19} \text{ m}^2$; $n \approx 8$

As indicated by the parameter n (Chapter 4.3) the slope of the corresponding permeability/porosity relationship is much steeper for wet conditions than in the dry state, i.e., the sealing efficiency during reconsolidation is much better.

- the permeability of clay/salt mixtures lies several orders below the bands for dry and wet crushed salt.

For example at $\Phi = 10\%$ $\Rightarrow k_{\text{crushed salt-dry}} > 1 \cdot 10^{-14} \text{ m}^2$

$\Rightarrow k_{\text{crushed salt-wet}} > 8 \cdot 10^{-16} \text{ m}^2$

$\Rightarrow k_{\text{clay/salt mixture - dry}} \approx 2 \cdot 10^{-16} \text{ m}^2$

$\Rightarrow k_{\text{clay/salt mixture - wet}} \approx 1 \cdot 10^{-19} \text{ m}^2$ to $< 10^{-21} \text{ m}^2$

In addition, **Figure 4.4** shows the slope for the clay/salt curves is much steeper than for crushed salt, varying between $n = 10$ to 19 .

Despite the observed scattering and “lithological” differences the permeability data are remarkably consistent and provide a basis for defining the upper and lower bounds of crushed salt permeability during time- and stress-dependent reconsolidation.

Because natural salt always contains small amount of fluids, the most relevant sets are those measured with brine (here described as *wet*). Testing with moistened or wet salt is more relevant to in situ conditions because long-term consolidation of crushed salt in an underground repository is facilitated by small amount of accessible moisture. The long-term mechanism giving rise to grain boundary healing is identified as fluid assisted diffusional transfer by Spiers et al. (1988).

Thus it follows that permeability data measured during “dry” crushed salt compaction or using “dry” nitrogen or oil for measuring permeability are not representative of the in situ state because the action of physico-chemical deformation processes at grain boundaries are suppressed, i.e., only plasticity and intra-crystalline gliding processes are acting.

5 NATURAL ANALOGUES / FIELD-SCALE OBSERVATIONS / APPLICATIONS

5.1 Introduction

Both experimental and micro-mechanical process understanding demonstrate support of waste disposal in salt formations, because disaggregated salt can be reconsolidated to sufficient densities to prevent excavated openings from becoming preferred pathways for transport and possible release of hazardous materials. However, disparity of both time and geometric scales is a recurring criticism of laboratory reconsolidation testing a valid concern in licensing a nuclear waste repository in salt. The question of extrapolating experimental data obtained from lab test research arises because small-scale phenomena may only be representative of limited size and relatively short test duration. Field-scale observations and analogues can help connect laboratory results to full repository scale applications. In addition, micro-mechanical observations are essential to demonstrate that the same deformation processes are acting independent from the investigation.

Analogue comparisons of many types may be important within the framework of a safety case. As an example, a specific topic of the German project ISIBEL (ISIBEL, 2010) identified and assessed natural analogue applications to the salt repository safety case. We expect analogue arguments will be necessary to establish safety functions inherent in the licensing process. Although analogues are imperfect renditions of salt repository seal elements, long-term processes and properties of the underground workings can be related to the functionality of salt repository seal systems. **Figure 5.1** depicts several occurrences of natural and anthropogenic analogues. Examples include back filling measures in ancient salt mines, such as the bronze age workings in Austria (**Figure 5.1 a**) (<http://www.archaeologie-online.de>), convergence of old back-filled drifts in the Asse salt mine (**Figure 5.1 b**), geological analogues such as damage healing evidenced in the photomicrograph shown in **Figure 5.1 c**), and natural diagenesis of salt deposits shown in **Figure 5.1 d**) from Warren (2005).

5.1.1 Anthropogenic analogues

Figure 5.1 a) is a photograph of reconstruction work ongoing at the Dürrenberg salt mine. Hallstatt and Dürrenberg are two of the world's first known salt mines. These mines, dating back thousands of years, provide direct evidence of preservation provided by salt and indirect evidence of no flow. Archeological evidence of salt healing includes intact Celtic miners, wood braces, rope, ruck sacks and other manmade articles. Further evidence of long-term salt encapsulation via closure and healing can be obtained from old salt mines such as these.

5.1.2 Technical analogues

Conventional salt mining activities have been ongoing in deep salt mines for over 100 years. Salt backfill has been placed in these old workings of conventional salt or potash mines to slow down time-dependent damage and failure of load bearing pillars by providing confinement and support for the rock mass, thereby limiting the amount of convergence. Examples for backfill measures with crushed salt exist in the Werra- and South Harz-Area of Germany. Sometimes also refinery waste (heated salt tailings) has been stowed. **Figure 5.1 b)** is a photograph of the long-term deformation in the Asse potash mine, which was in production in the early 1900s.

5.1.3 Healing and sealing the EDZ

Additional investigation opportunities result from the time-dependent compaction of cataclastic aggregates created by brittle deformation processes around underground opening. **Figure 5.1 c)** illustrates healing created by convergence-induced self-acting compaction process during cavity closure. Local damage or dilatancy (creating several percent of porosity) around excavations is a common feature in the operational phase in salt mining. After backfilling loading conditions will change to non-dilatant, crack closure and subsequent healing will take place, and the initial tightness of the salt will be restored. These phenomena are clearly documented by results from lab testing as discussed elsewhere (e.g., Popp et al. 2012b) and substantiated by field investigations (e.g., Wieczorek and Schwarzianeck, 2004, Bechthold et al. 2004). Due to time dependent self-sealing, the disturbed salt permeability decreases in short time scales to the initial state of rock tightness. In the EC project THERESA, dilatancy and recompaction of rock salt was the topic of a modeling exercise with a dedicated lab test (Wieczorek et al. 2009). In addition, the demonstration of cohesion between former shear planes between salt blocks confirms the action of healing (Salzer et al. 2007).

5.1.4 Geologic analogues

Diagenesis of natural salt changes primary deposits of high-porosity evaporate crystals in brine seaways or lakes into consolidated salt rocks with negligible porosity (**Figure 5.1 d)**). Processes of evaporite rock formation at low temperatures and pressures are reflected in grain size and texture changes due to crystal growth, recrystallization, back reactions and replacements in the salt matrix, accompanied by fluid squeeze off, as long as the effective porosity is not occluded by compaction and secondary evaporite cementation. The pervasive early loss of porosity from more than 50% near the surface to essentially zero by 100m depth is well documented in various studies (e.g., Warren, 2006). For instance, Casas and Lowenstein (1989) showed that Quaternary halite layers only 10 m below the land surface have typical porosities of <10% and that layers at depths below 45m are lightly cemented without visible porosity. By 100m of burial, almost all the halite units were tight and impervious.

Further analogue studies are recommended to reinforce conclusions drawn here. Although several examples of mining-induced compacted salt backfill are available, they are rarely perfect analogues. The geotechnical setting usually includes some deficits that have to be taken into account during data interpretation, e.g., representative material, knowledge about initial state and stress and deformation history.

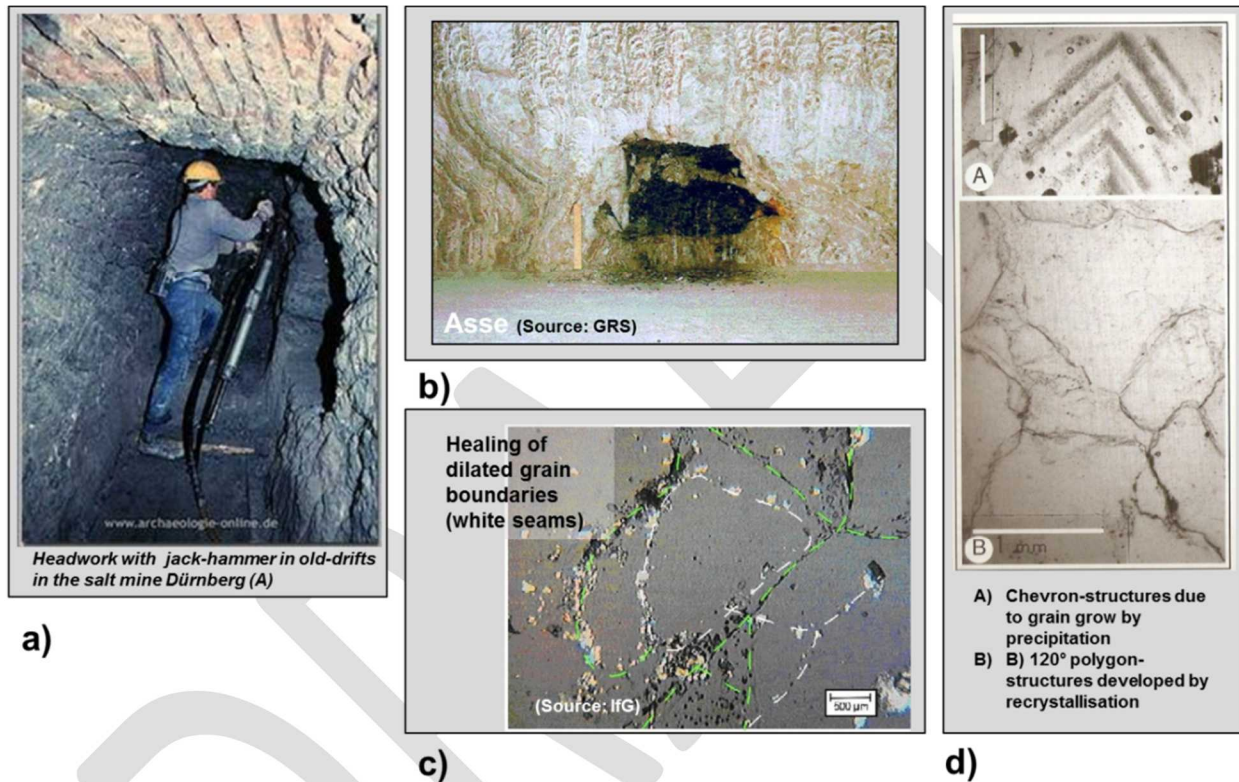


Figure 5.1 Summary of analogues.

5.1.5 Underground Research Laboratories (URL's)

URL's with generic or site- and material-specific investigations provide the scientific and technical information and practical experience that are needed for the design and construction of nuclear waste disposal facilities (NEA, 2001). An overview of URL's where investigations with backfill measures using crushed salt were performed is given in **Table 5.1** (Kuhlmann and Sevougian, 2013). In addition to the tests which have been performed at the WIPP site, perhaps the best documented and most relevant examples of a full-scale backfill demonstration project at a generic URL was the BAMBUS project at the Asse mine, which will be discussed further. Full-scale testing within a URL could allow evaluation of construction techniques, large-scale

demonstration of admixtures, such as bentonite, and achievable short-term performance measures.

DRAFT

Table 5.1. Underground research labs in salt formations with backfilling investigations.

Site	Test/Experiment	Period
Asse mine (Germany): Permian rock salt - anticline at various depth levels between 490 and 975 m	Thermal Simulation of Drift Emplacement (TSDE)	1990 – 2000
	Post Test Analysis of the TSDE experiment (BAMBUS)	2000 – 2004
	DEBORA-Project (Development of Seals for high-level (radioactive) waste disposal boreholes)	1991 – 1995 (Phase I) 1996 – 1999 (Phase II)
WIPP (USA): Permian bedded salt deposit at a depth of 655m	Heated canister backfill	1985 - 1988
	Seal system performance tests for various seal materials (Room M)	1985 - 1988
	Shaft sealing crushed salt reconsolidation	1993 - 1996
Amélie mine (France): Tertiary bedded salt: at a depth of 520 meters	Several borehole heater tests with crushed salt backfill with different grain size distributions	1986 -1999

5.1.6 WIPP Shaft Seal

In advance of the submittal of the Compliance Certification Application for the Environmental Protection Agency's license to operate, Sandia National Laboratories developed, demonstrated and modeled shaft seal performance in the WIPP setting (Hansen and Knowles, 1999). Reconsolidation of compacted mine-run salt in the shaft was an essential component of the WIPP compliance shaft seal design. The proposed use of granular salt as a functional seal element in the WIPP shafts gave rise to several technological advances, ranging in applicable scale from scanning electron microscopy of dislocation substructures to large-scale dynamic compaction of 40 m³ of mine-run salt.

A large-scale dynamic compaction demonstration using mine-run WIPP salt (Hansen and Ahrens, 1996) established possible initial conditions of a compacted salt seal component. Hansen and Ahrens selected deep dynamic compaction as a construction technique because it provides the greatest energy application to the crushed salt of available techniques, is relatively easy to apply, and has an effective depth of compactive influence far greater than lift thickness (approximately

2 m). Transport of granular salt to the working level in a shaft can be accomplished by dropping it down a slickline. If desired, a small mist of additional water can be sprayed onto the crushed salt as it is placed at the shaft working horizon. The basic construction technique was demonstrated above ground; however, the concept is readily adaptable to existing shaft backfilling procedures.

The large-scale dynamic compaction demonstration using mine-run salt produced a compacted mass having a fractional density of 0.90 and a permeability of $9 \cdot 10^{-14} \text{ m}^2$. Modeling evolution of crushed salt from these initial conditions to a high-density, low permeability seal required implementation of a suitable constitutive model, which was developed by Callahan (1999). Using reconsolidated salt as a repository sealing element requires refinement of model parameters, definition of the relationship between permeability and density and a solid understanding of the micromechanical process. Implementation of a proper constitutive model, inclusion of a reliable permeability/density relationship for reconsolidating crushed salt, and a fundamental understanding of micromechanical processes assure credible design and analyses of the WIPP shaft seal system.

To enhance compaction, nominally 1 wt. % water was added to the mine-run salt. The large-scale compaction demonstration produced 40 m^3 of compacted salt that had a uniform fractional density equaling 0.90 of natural intact salt. These results established the datum for shaft construction and basis for initial conditions of laboratory investigations. The permeability of compacting crushed salt is known to decrease as density increases (i.e., void ratio decreases) (Brodsky, 1994) and the density of crushed salt in the seal increases with time as the shaft diameter naturally closes. An example of reconsolidation test results is given in **Figure 5.2**. Test conditions included hydrostatic confining stress of 1 MPa and a pore fluid inlet pressure of 0.35 MPa. Two of the four curves on **Figure 5.2** represent actual test measurements; the other two are calculated. The curve labeled "Burette Measurement" is the total measured volume of brine collected at the vented end of the specimen, and the curve labeled "Volumetric Strain" is the test system measurement provided by a dilatometer. The data indicate that the saturated specimen is compacting; thus some volume of brine is being expelled from the vented end. The burette measurement has two components. One is the volume being expelled by consolidation, and the other is the volume of fluid migrating through the specimen. When the volume of expelled pore fluid derived from consolidation is subtracted from the burette measurement, the apparent permeability is found to decrease rapidly from an initial value of about $5 \cdot 10^{-16} \text{ m}^2$ to zero flow after 10 days. Experimental difficulties, such as a plugged brine flow tube, could account for apparent loss of permeability. Therefore, as the test apparatus was disassembled, the confining pressure was carefully reduced to allow flow around the specimen, which demonstrated that no

restriction to flow developed except for that presented by the specimen itself. Based on these convincing test results and results obtained by Brodsky (1994), it appears that brine permeation through dense reconsolidating salt is self-limiting.

DRAFT

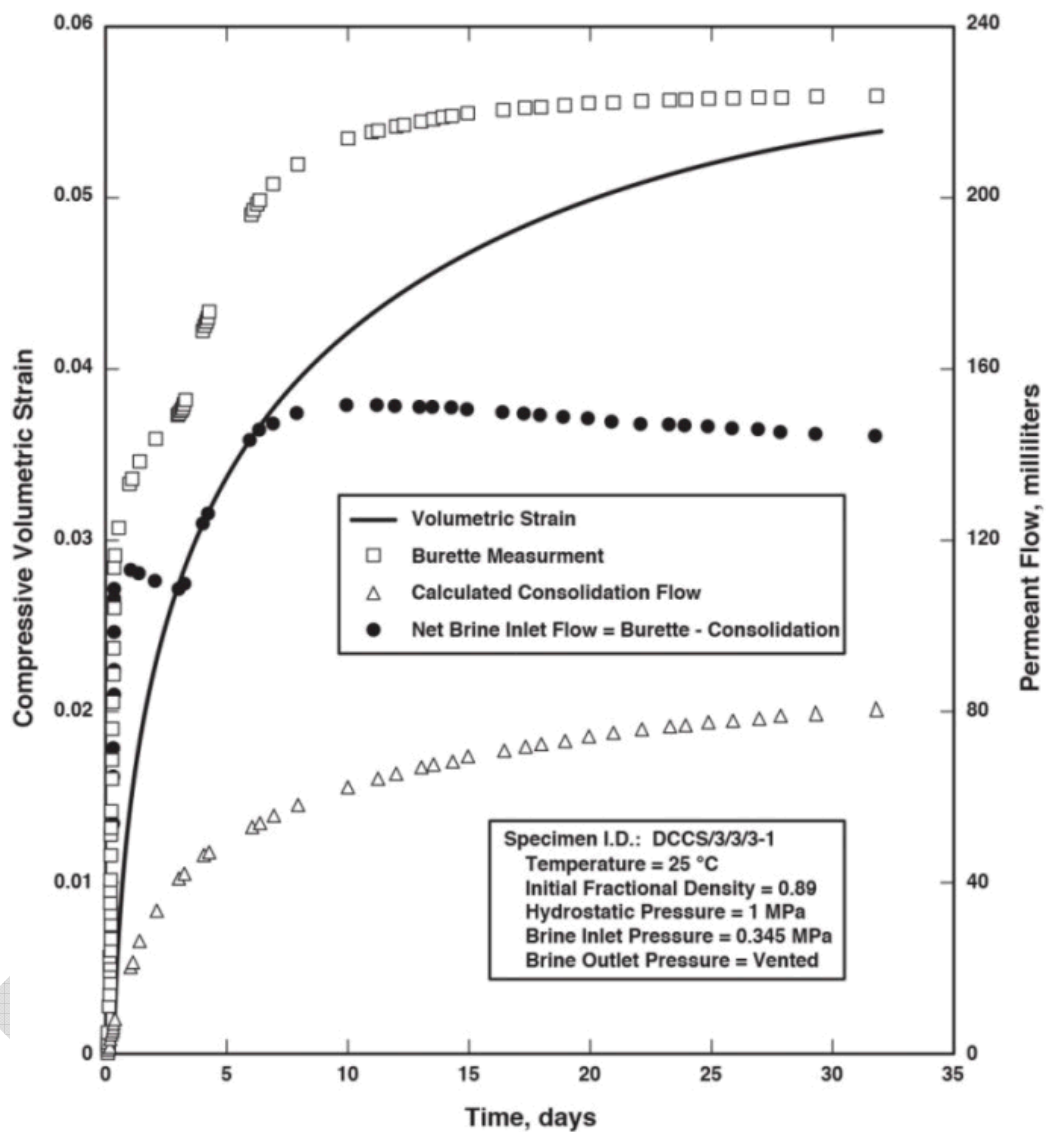


Figure 5.2 Volumetric Strain and Brine Flow Measurements on Reconsolidating Granular Salt.

In thin sections made after reconsolidation, a large percentage of the initial fine powder was removed by pressure-solution and re-precipitation (Brodsky et al. 1996). Confirmation of microprocesses was made by scanning electron microscopy as shown in the photomicrographs in **Figure 5.3**. The initial state of dynamically compacted salt in the left micrograph exhibits loose grain boundaries, while post-consolidation substructures in the right micrograph are sutured by pressure solution re-deposition. The porosity of the tamped salt on the left is 10%, while the reconsolidated and impermeable porosity on the right is 2%. In addition, the fracture face

exposed in the SEM showed grain boundary separation in the compacted salt and grain cleavage in the reconsolidated salt. The nature of the fracture surfaces demonstrated that the strength of grain boundaries after pressure-solution/precipitation is sufficient to favor crystalline fracture along cleavage planes rather than fractures along grain boundaries.

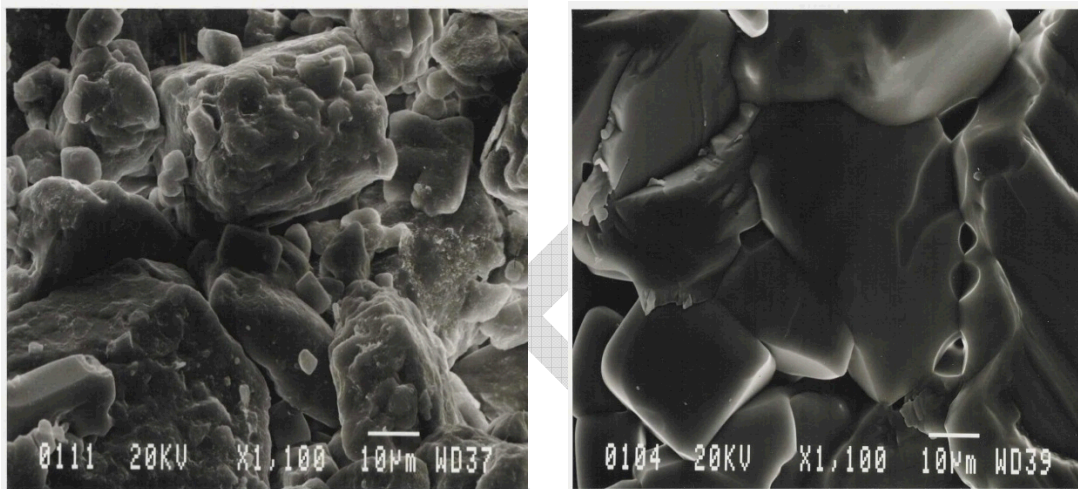


Figure 5.3 Dynamically compacted WIPP salt (left), reconsolidated WIPP salt (right).

In summary, the construction demonstration using dynamic compaction showed that an initial density of 0.90 could be obtained readily. Ambient laboratory reconsolidation of the compacted salt demonstrated that porosity and permeability were reduced dramatically under modest stress conditions. Post-test microscopy documented the mechanisms by which the tamped salt reconsolidated. This research convinced the independent regulatory authority that reconsolidation of granular salt thus compacted in the shaft would attain high performance in its functional setting.

5.2 Drift closure

5.2.1 BAMBUS II – mockup-test

The BAMBUS and BAMBUS II Project (Bechthold et al. 2004) provide the best available full-scale, long-term, thermomechanical information on granular salt reconsolidation at in situ conditions. The principal scientific objective of the project was to extend the basis for optimizing the repository design and construction and for predicting the long-term performance of barriers, including the reconsolidation of crushed salt backfill.

In situ investigations were carried on in the Asse salt mine subsequent to completion of the large-scale Thermal Simulation of Drift Emplacement (TSDE). The TSDE (also discussed in Bechtold

et al. 2004) involved an emplacement drift that was electrically heated to between 170 and 200°C for more than 8 years. Sandia was a partner on the BAMBUS II in situ reconnaissance and performed permeability tests and petrofabric microscopy on the reconsolidated salt. The photograph shown in **Figure 5.4** is the BAMBUS II setting as the test room was re-entered. The large heater is surrounded by reconsolidated granular salt, which had various porosities depending upon location. Most porosity measurements ranged from 20 to 25%. Initial porosity was approximately 35% in 1990. After ten years of in situ reconsolidation, porosity was reduced by 10 to 15% and closure rate had levelled off at 0.5% per year. An additional 20 years or more under these conditions would be required to reduce the porosity sufficiently to produce a low permeability medium.



Figure 5.4 Photograph of the BAMBUS II re-excavation.

Characterization of the reconsolidated salt included microstructural petrofabrics and laboratory tests. The photomicrographs in **Figure 5.5** are a thin section in cross-polarized light (left) and surface image from a SEM (right). These photomicrographs were on specimens prepared directly from BAMBUS II salt extracted as shown in the field test photograph **Figure 5.4**. This particular sample has a measured porosity of 20.7% and a permeability of $4.2 \cdot 10^{-13} \text{ m}^2$ which is on the low end of other measurements on the BAMBUS II project (more typically 10^{-11} m^2). Brittle processes dominate, as can be seen from the small, sharply angular grains situated between larger

grains, all of which exhibit cubic cleavage. The grain boundaries are not sutured as evidenced by the fracture surface in **Figure 5.5 b)**. The grains have minimal evident cohesion when broken, as breakage was accommodated at the grain boundary and not through the grains. Grain boundaries show no evidence of healing processes and the flexural breakage was accommodated by separation of grain boundaries and not tensile failure of the grains themselves.

DRAFT

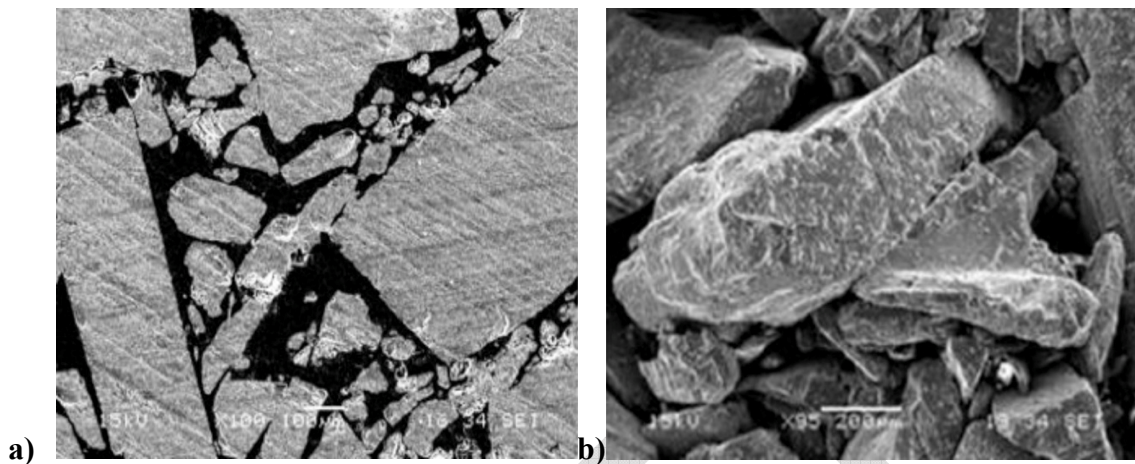


Figure 5.5 Micro-structures of consolidated Salt with 20.7% Porosity.

The BAMBUS II reconsolidated salt having 20.7% porosity measured permeability in the range of 10^{-13} m² or higher while the dynamically compacted WIPP salt having a porosity of 10% exhibited approximately 10^{-14} m² permeability. These porosities and permeabilities are relatively high with respect to ultimate performance expectations for reconsolidated salt as backfill or seal system elements in a salt repository. In that respect, the functional relationship is most important when porosity is <10%, particularly when the permeability approaches the very low values of the native rock salt.

5.2.2 Operating Mines - Crushed salt properties and microstructural observations

Structural stability is often achieved in the salt and potash industry by backfilling excavations. Backfilling is performed for operational efficiencies and seldom are the physical or mechanical properties of the backfill measured. Two forensic examinations are presented here, recognizing that further anthropogenic analogue studies are strongly desired. On one technical visit to the Sigmundshall K + S mine, a sample of reconsolidated slurry was obtained from the mine workings. This sample had a very low porosity (1.4%) and an approximate permeability of 10^{-17} m² (Bechthold et al. 2004). Sutured intergranular structures are ubiquitous, produced by the introduction of large amounts of water when the slurry was placed and assisted by ongoing pressure solution redeposition. This analogue demonstrates that slurry will reconsolidate to near intact conditions in the working life time of a mine.

Other samples of a younger slurry backfill operation were obtained from the Canadian K2 mine. The reconsolidated K2 salt was originally deposited by slurry from the surface in 1988 (Kaskiw et al. 1989). The slurry was approximately 30% solids consisting of salt tailings. Excess brine decanted by gravity out the back end of very slightly dipping room (less than 0.05% slope).

Rooms were filled completely with slurry. Room closure rate was measured at 1-2 inches per year in rooms 25 feet wide and 12 feet tall. Intact cubes measuring approximately 4 inches on a side were obtained for optical microscopy to evaluate the reconsolidation process. In this particular case the closure has occurred over some 30 years at a rate of 1-2 inches per year: between 20% and 40% of the total void space has been removed.

Figure 5.6 includes two photomicrographs of the reconsolidating slurry extracted from the K2 Mine after 30 years. On the left, approximately 50% of the field of view is epoxy, which is easily differentiated from the cubic salt grains. The epoxy is lighter shade and exhibits light scratches from polishing. The field of view is 1 mm across, a magnification of approximately 100 X, approximately the same as the SEM photomicrographs in **Figure 5.5**. Notice the exceptional suturing of grain boundaries. Wherever the grains are in contact, the boundaries mesh perfectly because the ample water available promotes pressure solution and re-deposition. There are no apparent crystal plasticity or brittle processes active. The grains nicely accommodate movement of mass at the contact surfaces. This is particularly notable in the triple junction at the upper center of the field of view a). The substructures in the photomicrograph on the right b) exhibit greater grain density, although these micrographs are shot only a few centimeters apart. The photomicrograph shows the detail of grain boundary healing and consumption of the fine grains along the closing of the contact zone.

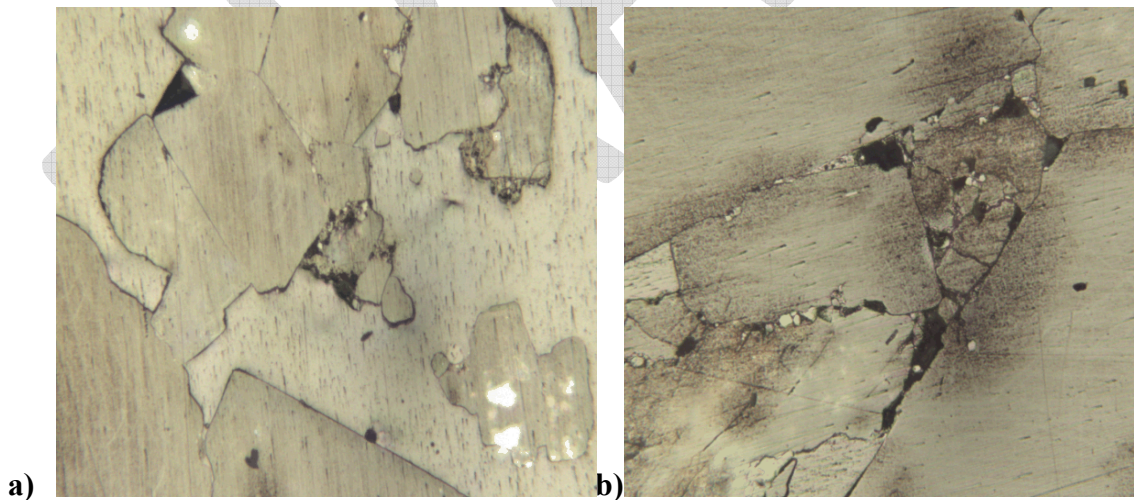


Figure 5.6 Reconsolidation of slurry backfill at the K2 mine after 30 years.

Reconsolidation of granular salt has practical structural and production implications in salt mines, such as the K2 mine. In repository applications, permeability would be the primary attribute of

concern. In this field example we note that grain boundaries mesh extremely well and would be impermeable at that boundary. As natural creep closes the room, the remaining water is expelled as the pressure solution re-deposition removes the void space. The process of reconsolidating salt here is analogous to the process by which the Permian Basin bedded salt became an impermeable formation, originating as embayed salt slurry choked with hopper crystals. For repository closure systems, panel closures would be constructed by utilizing engineering techniques to achieve low emplacement porosity. However, it is also important to recognize that fluid slurry will consolidate to intact conditions.

5.2.3 Convergence - Drift closures at WIPP

In the US, ambient reconsolidation was studied principally in terms of design, construction and performance of shaft seal system elements for the WIPP. By contrast, drift seal system elements have a more challenging orientation, which is less favorable for initial construction. Initial construction proficiency and optimization with possible additives should ensure short-term attainment of an impermeable state. As of the writing of this review paper, there remains a need to understand properties of the backfill upon construction and as a function of time shortly thereafter. Significant research has been undertaken and this issue persists as a topic of great interest to international salt repository research, design and operations.

As a case in point, today there is renewed interest in salt reconsolidation as applied to drift closures at the WIPP. The outcome of ongoing waste disposal panel closure redesign could establish a basis for backfilling and drift closures associated with repository design for disposal of heat-generating nuclear waste. The WIPP panel closure redesign concerns analysis of the time-dependent reduction in fractional density, porosity and permeability of run-of-mine granular salt emplaced in a salt drift excavation. Multiple analyses used calculations with a creep consolidation model, supported by laboratory data and field experience. Estimates of reconsolidation were made in a series of calculations by Herrick (2012), which identifies the codes and models used. Simulations started with the crushed salt placed initially porosity of 15%, 20%, 25%, and 33%. Given the boundary conditions and parameters employed by Herrick, a porosity of 5% was achieved between 40 and 140 years from an initial porosity of 15% and 33%, respectively. This example displays the inherent uncertainty introduced with numerical modeling. Results of many different magnitudes can be calculated, but regulators and operators often require performance metrics with tighter tolerances and greater certainty.

As noted by Hansen and Thompson (2002), an engineering estimate of closure time can be made using accumulating data for WIPP entries. Measurements of roof-to-floor and rib-to-rib closure in the waste disposal panel entries indicate closure rates have remained stable and uniform for more than 20 years, as shown in **Figure 5.7** (US DOE, 2011). Projected forward, the volume closure

equates to about 1% per year. A volume closure of 30% increases the fractional density from 67% to 96% and decreases the porosity from 33% to 4%. Thus, based on engineering estimates, granular salt would return to low porosity in thirty years. Hansen and Thompson (2002) cautioned that slower reconsolidation might be expected as back pressure develops. There are several mitigating arguments that ensure tight panel closures in a reasonably short operational period. The first is that the in situ closure rates shown **Figure 5.7** are the slowest observed in the WIPP underground. Equivalent panel entries further south are situated 2.43 m higher in the stratigraphy and are closing at twice the rate, which would achieve low porosity and low permeability in half as much time. A second scientific argument for tight panel closures in a few decades comes from test results that show reconsolidation to occur rapidly at low stress conditions (for example see **Figure 5.2**) and that backpressure effects would be minimal. It is entirely possible to construct a lateral closure to relatively high density and such demonstrations in a URL would be very beneficial to salt repository design, operations and performance.

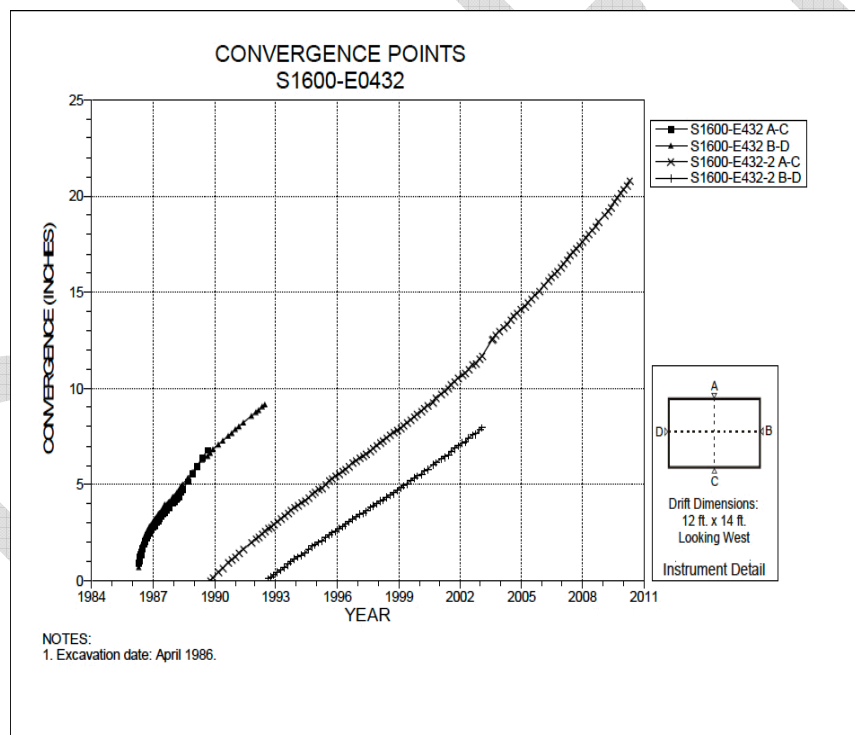


Figure 5.7 Closure measurements Panel 1 entry.

5.2.4 Preliminary safety analysis Gorleben (VSG)

The project VSG which involved all German institutions working in the field of repository research had the objectives to

- Develop a systematic compilation of knowledge on the Gorleben site
- Identify remaining research needs, both site specific and site independent
- Develop methodologies for summarizing and evaluating knowledge to be used in future site selection processes
- Investigate the transferability of disposal and sealing concepts to repository systems in other host rocks than salt

Among others, the work schedule comprised modeling of gas/brine flow (Kock et al. 2012) and contaminant dispersal (Larue et al. 2013) in the repository system. Since, according to the German disposal concept, the disposal drifts or boreholes as well as the access drifts will be backfilled with granular salt, a prediction of the crushed salt compaction with time under various conditions was necessary. These conditions included

- High temperature, dry crushed salt with an initial porosity of 35% in disposal drifts
- Ambient or moderately increased temperature, crushed salt with an initial porosity of 35% and a small moisture content (0.6 – 1%) for acceleration of recompaction in access drifts
- Ambient temperature, precompacted granular salt (10% initial porosity) with a moisture content of 1.5% as part of the shaft seal (long-term seal)

Simulations were performed using the constitutive models implemented in the finite element simulator CODE_BRIGHT (Olivella and Gens, 2002), which include the deformation mechanisms elasticity, viscoplastic deformation by grain crushing/reorganization, dislocation creep, and fluid assisted diffusional transfer (compare to **Figure 2.1**). Parameters were calibrated from the laboratory tests shown in **Figure 3.5**, which continues but has not reached the interesting low porosity range at the time of this writing. For the granular salt in drifts, the calculations estimate between 10 and 200 years will be needed to compact to porosity below 5%, depending on the boundary conditions (Czaikowski and Wieczorek, 2012). A calculation considering dry crushed salt at ambient temperature estimated 1000 years would be required for reconsolidation below 5%. Depending on the assumed creep properties of the adjacent rock, similar calculations for the shaft seal estimated 200 – 1000 years would be needed to attain a final porosity of 1% (Müller-Hoeppe et al. 2012).

6 PERCEPTIONS / FUTURE WORK

The technical basis or state of knowledge regarding granular salt reconsolidation is mature. Crushed or run-of-mine salt makes an excellent backfill material for salt repositories because its healing properties will ultimately reestablish impermeability to brine flow and radionuclide transport. By virtue of creating underground space, mine-run salt is readily available and relatively easy to emplace in drifts, although high emplacement density in a horizontal configuration remains an engineering challenge. A large number of laboratory and in situ tests have been conducted to determine the properties of crushed salt under a wide variety of conditions. The science supporting the technical basis for properties of reconsolidating granular salt is objective and thorough. Despite the foundation of supporting evidence, the repository licensing process requires scientific evidence to be conveyed to stakeholder and regulators in a fashion that simultaneously demonstrates the supporting information and convinces a nontechnical audience.

During the 3rd US/German workshop on salt repository research, design and operation (Hansen et al. 2013), a questionnaire was distributed regarding the role of crushed salt in repository science to which 16 salt-expert responses were received. One question asked whether all the relevant processes in crushed salt reconsolidation have been considered. Responses were generally positive, but not convincingly high, which indicates that even a learned population believes that additional research is necessary to characterize reconsolidation of granular salt fully. Permeability was acknowledged as the most important attribute associated with repository application, followed by mechanical and thermal properties. Some areas of uncertainties were identified:

Test scale. Testing time and space scales need to be reconciled with the desired predictions for repository applications. Laboratory tests comprising the bulk of empirical evidence are principally small-scale and short duration; whereas the application involves meter scale drifts and times ranging from year operations to perhaps hundreds of years.

Additives. Most backfill research and design now uses run-of-mine crushed salt without additives such as bentonite. Evidence suggests that performance characteristics could be improved with admixtures. Admixtures provide greater placement density and performance. This engineering achievement reduces uncertainty and perceived reliance on modeling.

Characteristics at low-porosity. Determining permeability at low porosity presents difficult experimental conditions. The technical basis for the crucial transition to low permeability could benefit from further study.

The results of this survey were illuminating. A group of salt practitioners was equivocal in their degree of confidence in current model calibrations related to granular salt reconsolidation. Self-identified *experts* responded with higher confidence than *non-experts*. Whereas some technical experts believe the phenomena associated with crushed salt reconsolidation are well understood, it is clear that this view is not held by other experts and informed lay personnel. The perception that salt reconsolidation processes and associated phenomena are imperfectly known is vital to license application for a salt repository. A regulatory authority will ultimately weigh the objective evidence and decide the merit of performance arguments. In consideration of our own high expectations for scientific rigor, continued research on reconsolidation of granular salt remains a focus of US/German collaborations.

Given these perceptions, we put forward the following questions, observations, and recommended activities:

- What final porosity of crushed salt is necessary to achieve an efficient seal and at which time can it be reached?

This topic has been controversial in the past because most oedometer tests demonstrate a residual porosity on the order of 5%. The test results seem to contradict the assumption of a final negligible porosity within a limited time scale. A preponderance of technical information provided within this document clearly demonstrates that granular salt can achieve final porosity on the order of 1% within 10 to 50 years due to time dependent consolidation processes. These processes may have been neglected somewhat in past research, which focused more on the stress-dependent compaction. However, differences between tests performed in an oedometer-equipment and triaxial tests are apparent and the experimental variability should be elaborated upon as future experimental work is considered.

- Capability of additives such as moisture and clay can be optimized for construction and attainment of sealing properties.

It is well known that small amounts of moisture can enhance the salt compaction and reconsolidation, but the optimal content remains in question. Apparently, added moisture less than 1% is very effective. But what is the optimal moisture addition if the granular salt is mixed with clay? The potential of possible additives for improving backfill and sealing properties has not been exhausted.

- The nature of testing fluids (brine or gas) and the resultant permeability/porosity relationships warrant further examination.

Although up to now only few data are available, the results document that the decrease of permeability is more effective if brine is the test fluid. In addition, if bentonite is added the compacted backfill becomes tighter. That means it is not possible to derive a unique permeability/porosity relationship for granular salt with and without additives. The apparent differences result from physico-chemical processes on the grain scale, i.e., permeability is not only a function of mechanical pore space compaction.

- Numerical modeling provides capabilities but lacks low porosity verification:

Several numerical tools and models are available for calculations involving reconsolidation. However, the codes need to be qualified for characteristics appearing at lower porosities, i.e., <5% based on the experimental results. Model evaluations of backfill reconsolidation were important to the VSG safety analyses. Questions remain regarding effects of humidity in the long term, transport parameters, and the role of two-phase flow.

- Further analogue experiences from underground sources is imperative.

Revisiting the BAMBUS II site after more than 10 years additional years of natural reconsolidation is strongly recommended and seems to be possible. We suggest core sampling, permeability testing, microscopy, further reconsolidation in the laboratory, and hydro-frac testing. In addition, the salt repository community should continue to pursue relevant information from forth-coming projects for abandoning conventional mines. A large-scale in situ application of pre-compacted granular salt/mixture as an impermeable element for shaft sealing will be realized for the shaft Saale (former potash mine Teutschenthal, Germany) probably within the next 5 years. The technical preparation is in progress.

Large data bases support reconsolidation of granular salt to low porosity and very low permeability, which equate to undisturbed native salt. This review has summarized the existing information with a view toward salt repository applications. The role of granular salt reconsolidation in a repository for heat-generating waste will vary among programs because attainment of the safety functions depends on the natural setting, the waste inventory and the concept of operations. Contingent on the repository design and safety concept, reconsolidating crushed salt can function well as a sealing material in shafts or drifts depending on construction techniques and time-dependent tightness evolution. Empirical evidence provides high confidence for excellent reconsolidation performance because processes are well understood and achievable with practical engineering measures.

7 REFERENCES

- Beauheim, R.L., and R.M. Roberts (2002), "Hydrology and Hydraulic Properties of a Bedded Evaporite Formation," *Journal of Hydrology*, 259, pp. 66-88.
- Bechthold, W., T. Rothfuchs, A. Poley, M. Ghoreychi, S. Heusermann, A. Gens, and S. Olivella (1999), Backfilling and Sealing of Underground Repositories for Radioactive Waste in Salt (BAMBUS Project). Final Report. European Commission, Call No.: EUR 19124 EN, Brussels.
- Bechthold, W., E. Smailos, S. Heusermann, T. Bollingerfehr, B Bazargan Sabet, T. Rothfuchs, P. Kamlot, J Grupa, S. Olivella, and F.D. Hansen (2004), Backfilling and Sealing of Underground Repositories for Radioactive Waste in Salt (BAMBUS II Project): Final Report. European Commission. Directorate General for Research. Office for Official Publications of the European Communities. Call No: EUR 20621 EN.
- Brodsky, N.S. (1994), Hydrostatic and Shear Consolidation Tests with Permeability Measurements on Waste Isolation Pilot Plant Crushed Salt. SAND93-7058, prepared by RE/SPEC Inc., Rapid City, SD, for Sandia National Laboratories, Albuquerque, NM.
- Brodsky, N.S., F.D. Hansen, and T.W. Pfeifle (1996), Properties of Dynamically Compacted WIPP Salt, Proceedings of the 4th International Conference on the Mechanical Behavior of Salt, Montreal, Quebec, Canada, June 17-18, 1996. SAND96-0838C. Albuquerque, NM: Sandia National Laboratories.
- Broome, S., S. Bauer, and F. Hansen (2014), Reconsolidation of Crushed Salt to 250°C under Hydrostatic and Shear Stress Conditions. American Rock Mechanics Association, Minneapolis, MN. SAND2014-1371C. Albuquerque, NM: Sandia National Laboratories.
- Callahan, G.D., M.C. Loken, L.D. Hurtado, and F.D. Hansen (1996). Evaluation of Constitutive Models for Crushed Salt. The Mechanical Behavior of Salt IV: Proceedings of the fourth Conference, (MECASALT IV) Montreal, edited by M. Aubertin and H.R. Hardy Jr., Trans Tech Publ., Clausthal, Germany.
- Callahan, G.D., K.D. Mellegard, and F.D. Hansen (1998), "Constitutive Behavior of Reconsolidating Crushed Salt," *Int. J. Rock Mech. Min. Sci.*, 35, No. 4-5, Elsevier.
- Callahan, G.D. (1999), Crushed Salt Constitutive Model. SAND98-2680. Albuquerque, NM: Sandia National Laboratories.
- Carter, N.L., F.D. Hansen, and P.E. Senseny (1982), "Stress Magnitudes in Natural Rock Salt," *Journal of Geophysical Research*, Vol. 87.

Casas, E., and T.K. Lowenstein (1989), "Diagenesis of Saline Pan Halite: Comparison of Petrographic Features of Modern, Quaternary and Permian Halites," *Journal of Sedimentary Petrology*, 59, pp. 724-739.

Case, J.B., P.C. Kelsall, and J.L. Withiam (1987), Laboratory Investigation of Crushed Salt Consolidation. 28th US Symposium on Rock Mechanics, Tucson, AZ.

Cinar, Y. (2000), Experimental Investigation on the Pore Structure and Fluid Flow in Artificially-Compacted Salt Granulates. Dissertation, Clausthal-Zellerfeld, 143 pp.

Cinar, Y., G. Pusch, and V. Reitenbach (2006), "Petrophysical and Capillary Properties of Compacted Salt," *Transport in Porous Media*, 64, pp. 199-228.

Czaikowski, O., and K. Wiczorek (2012), Salzgruskompaktion – Kalibrierung der in CODE_BRIGHT verwendeten physikalischen Modellansätze zur numerischen Simulation, Vorläufige Sicherheitsanalyse Gorleben (VSG), GRS Memorandum, 15.06.2012 (Rev. 30.08.2012).

Czaikowski, O., K. Wiczorek, and K.-P. Kröhn (2012), Compaction of Salt Backfill – New Experiments and Numerical Modeling. FKZ 02 E 10740 (BMW), The Mechanical Behavior of Salt VII: Proceedings of the 7th Conference (MECASALT VII). Paris.

Davidson, B., and M. Dusseault (1996), Crushed Halite Backfill as a Structural and Disposal Medium. The Mechanical Behavior of Salt IV: Proceedings of the fourth Conference, (MECASALT IV) Montreal, edited by M. Aubertin and H.R. Hardy Jr., Trans Tech Publ., Clausthal, Germany.

Davies, P.B. (1991), Evaluation of the role of threshold pressure in controlling flow of waste-generated gas into bedded salt at the Waste Isolation Pilot Plant (WIPP). SAND90-3246. Albuquerque, NM: Sandia National Laboratories.

Drury, M.R., and J.L. Urai (1990), "Deformation-related Recrystallization Processes." *Tectonophysics*, 172(3-4), pp. 235-253.

Elliger, C. (2004), Untersuchungen zum Permeationsverhalten von Salzlaugen in Steinsalz bei der Endlagerung wärmeentwickelnder nuklearer Abfälle, Dissertation, Technische Universität Darmstadt, D17.

Hansen, F.D. (1985), Deformation Mechanisms of Experimentally Deformed Salina Basin Bedded Salt. Battelle Memorial Institute. Office of Nuclear Waste Isolation. Columbus, OH. BMI/ONWI-552.

Hansen, F.D., and E.H. Ahrens (1996), Large-Scale Dynamic Compaction of Natural Salt. Proceeding of the 4th Conference on the Mechanical Behavior of Salt, Trans Tech Publications, Clausthal-Zellerfeld, Germany. SAND96-0792C. Albuquerque, NM: Sandia National Laboratories.

Hansen, F.D., and M.K. Knowles (1999), Design and Analysis of a Shaft Seal System for the Waste Isolation Pilot Plant. SAND99-0904J. Albuquerque, NM: Sandia National Laboratories.

Hansen, F.D., and T.W. Thompson (2002), Effective Permeability of the Redesigned Panel Closure System. Memorandum to Paul E. Shoemaker dated August 29, 2002. ERMS 523476. Albuquerque, NM: Sandia National Laboratories.

Hansen, F.D., S.J. Bauer, S.T. Broome, and G.D. Callahan (2012), Coupled Thermal-Hydrological-Mechanical Processes in Salt: Hot Granular Salt Consolidation, Constitutive Model and Micromechanics. FCRD-UFD-2012-000422, SAND2012-9893P. Albuquerque, NM: Sandia National Laboratories.

Hansen, F.D., K. Kuhlmann, W. Steininger, and E. Biurrun (2013), Proceedings of 3rd US/German Workshop on Salt Repository Research, Design, and Operation. SAND2013-1231P. Posted on the Sandia Workshop website: http://energy.sandia.gov/?page_id=17258.

Hellmann, R., J.R. Gratier, and T. Chen (1998), Mineral-water Interactions and Stress: Pressure Solution of Halite Aggregates. In Water-Rock Interaction WRI-9 (eds. G.B. Arehart and J.R. Hulston). A.A. Balkema, Rotterdam, pp. 777-780.

Hellmann, R., P.J. Renders, J.-P. Gratier, and R. Guiguet (2002), Experimental Pressure Solution Compaction of Chalk in Aqueous Solutions Part 1. Deformation Behavior and Chemistry Water-Rock Interactions, Ore Deposits, and Environmental Geochemistry: A Tribute to David A. Crerar. Eds.: R. Hellmann and S.A. Wood. Geochem. Soc., Spec. Publ. No. 7, 2002.

Herrick, C. (2012), Calculations Performed in Support of Reconsolidation of Crushed Salt in Panel Closures. Memorandum to WIPP Records Center. ERMS 557150. Albuquerque, NM: Sandia National Laboratories.

Holness, M.B. (Editor) (1997), Deformation-enhanced Fluid Transport in the Earth's Crust and Mantle. The Mineralogical Society Series, 8. Chapman & Hall, London.

Horseman, S.T. (2001), Gas migration through indurated clays (mudrocks). In: Gas Generation and Migration in Radioactive Waste Disposal. Proc. of the NEA Workshop in Reims 2000, France.

Hunsche, U., and O. Schulze (2001), Humidity Induced Creep and Its Relation to the Dilatancy Boundary. In: Basic and Applied Salt Mechanics; Proc. of the Fifth Conf. on the Mech. Behavior of Salt (MECASALT V), Bucharest 1999. Editors: N.D. Cristescu, H.R. Hardy, Jr., R.O.Simionescu; p. 73 – 87. Balkema, Lisse.

IfG (2012), Laboruntersuchungen am Gemisch Schnittsalz - Friedländer Ton. Institut für Gebirgsmechanik GmbH, Leipzig, 07.12.2012, 56 pp.

Ingram, G.M., J.L. Urai, and M.A. Naylor (1997), Sealing and top seal assessment. Hydrocarbon Seals: Importance for Exploration and Production. NPF Spec. Publ. 7, 165-174, Elsevier, Singapore.

ISIBEL (2010),

http://www.eurosafe-forum.org/userfiles/3_01_EUROSAFE2010_TowardsGermanSafetyCase_wol.pdf (2010)

Kansy, A. (2007), Einfluss des Biot-Parameters auf das hydraulische Verhalten von Steinsalz unter der Berücksichtigung des Porendruckes. Dissertation an der TU Clausthal, Clausthal Zellerfeld.

Kaskiw, L., R. Morgan, and D. Ruse (1989), Backfilling at IMC (Canada) K2 Potash Mines, Proc. 4th International Symposium on Innovation in Mining and Backfill Technology, Montreal QC.

Kock, I., R. Eickemeier, G. Frieling, S. Heusermann, M. Knauth, W. Minkley, M. Navarro, H.-K. Nipp, and P. Vogel (2012), Integritätsanalyse der geologischen Barriere, Bericht zum Arbeitspaket 9.1, Vorläufige Sicherheitsanalyse für den Standort Gorleben, GRS-286.

Kröhn, K.-P., D. Stührenberg, M. Herklotz, U. Heemann, C. Lerch, and M. Xie (2009), Restporosität und –permeabilität von kompaktierendem Salzgrus-Versatz, REPOPERM – Phase 1, Gesellschaft für Anlagen- und Reaktorsicherheit (GRS) mbH, GRS-254.

Kuhlman, K.L., and S.D. Sevougian (2013), Establishing the Technical Basis for Disposal of Heat-Generating Waste in Salt. FCRD-UFD-2013-000233. SAND2013-6212P. Albuquerque, NM: Sandia National Laboratories.

Larue, J., B. Baltes, H. Fischer, G. Frieling, I. Kock, M. Navarro, and H. Seher (2013), Radiologische Konsequenzenanalyse, Bericht zum Arbeitspaket 10, Vorläufige Sicherheitsanalyse für den Standort Gorleben, GRS-289.

McTigue, D.F. (1986), “Thermoelastic Response of Porous Rock,” *Journal of Geophysical Research*, Vol. 91, No. B9.

Müller-Hoeppe, N., M. Breustedt, J. Wolf, O. Czaikowski, and K. Wieczorek (2012), Integrität geotechnischer Barrieren, Teil 2 – Vertiefte Nachweisführung, Bericht zum Arbeitspaket 9.2, Vorläufige Sicherheitsanalyse für den Standort Gorleben, GRS-288.

Müller-Lyda, I., H. Birthler, and E. Fein (1999), Ableitung von Permeabilitäts-Porositätsrelationen für Salzgrus, GRS-148, Ges. für Anlagen- und Reaktorsicherheit, Braunschweig, Germany.

NEA (2001), The Role of Underground Laboratories in Nuclear Waste Disposal Programmes. OECD, Nuclear Energy Agency, Paris. 42 pps.

Olivella, S., and A. Gens (2002), “A Constitutive Model for Crushed Salt,” *Int. J. Numer. Anal. Meth. Geomech.*, 2002; 26, pp. 719-746.

Olivella, S., S. Castagna, E.E. Alonso, and A. Lloret (2011), Porosity variations in saline media induced by temperature gradients: experimental evidences and modelling. *Transport in Porous Media*, 90(3):763–777.

Paterson, M.S. (1973), “Nonhydrostatic Thermodynamics and Its Geologic Applications,” *Rev. Geophys.*, 11, pp. 355—389.

Peach, C.J., and C.J. Spiers (1996), “Influence of Crystal Plastic Deformation on Dilatancy and Permeability Development in Synthetic Salt Rock,” *Tectonophysics*, 256, pp. 101-128.

Popp T., and H. Kern (1998), “Ultrasonic Wave Velocities, Gas Permeability and Porosity in Natural and Granular Rock Salt.” *Physics and Chemistry of the Earth*, 23, pp. 373-378.

Popp, T., H. Kern, and O. Schulze (2001), “The Evolution of Dilatancy and Permeability in Rock Salt during Hydrostatic Compaction and Triaxial Deformation,” *J. Geophys. Res.*, 106 , No. B3, pp. 4061-4078.

Popp, T. (2002), “Transporteigenschaften von Steinsalz,” *Meyniana*, 54, pp. 113-129.

Popp, T., K. Salzer, O. Schulze, and D. Stührenberg (2012a), Hydromechanische Eigenschaften von Salzgrusversatz - Synoptisches Prozessverständnis und Datenbasis. Memorandum, Institut für Gebirgsmechanik (IfG), Bundesanstalt für Geowissenschaften und Rohstoffe (BGR): Leipzig, 30.05.

Popp, T., W. Minkley, K. Salzer, and O. Schulze (2012b), Gas Transport Properties of Rock Salt - Synoptic View, In: P. Berest, M. Ghoreychi, F. Hadj-Hassen, and M. Tijani, *Mechanical Behavior of Salt VII*, Taylor & Francis group, London N, ISBN 978-0-415-62122-9, 143-153.

- Raj, R. (1982), "Creep in polycrystalline aggregates by matter transport through a liquid phase," *Geophys. Res.*, 87 no. B6, pp. 4731-4739.
- Renard, F., D. Dysthe, J. Feder, K. Bjørlykke, and B. Jamtveit (2001), "Enhanced pressure solution creep rates induced by clay particles: Experimental evidence in salt aggregates," *Geophysical Research Letters*, Vol. 28, pp. 1295-1298.
- Renard, F., F. Bernard, X. Thibault, and E. Boller (2004), "Synchrotron 3D microtomography of halite aggregates during experimental pressure solution creep and evolution of the permeability," *Geophysical Research Letters*, Vol. 31, L077607.
- Salzer, K., T Popp, and H. Böhnel (2007), Mechanical and permeability properties of highly pre-compacted granular salt bricks. In K.-H. Lux, W. Minkley, M. Wallner and H.R. Hardy, Jr. (eds.), *Basic and Applied Salt Mechanics; Proc. of the Sixth Conf. on the Mech. Behavior of Salt. Hannover 2007*. Lisse: Francis & Taylor (Balkema), pp. 239-248.
- Schenk, O. (2006), *Grain boundary structure in minerals and analogues during recrystallization in the presence of a fluid phase*, Shaker, ISBN: 978-3-8322-5075-1, 172 pp.
- Schenk, O., J.L. Urai, and S. Piazzolo (2006), "Structure of grain boundaries in wet, synthetic polycrystalline. statically recrystallising Halite - evidence from cryo-SEM observations," *Geofluids* 6(1), pp. 93-104.
- Schutjens, P. (1991), *Intergranular pressure solution in halite aggregates and quartz sands: an experimental investigation*. PhD thesis, Universiteit Utrecht, 233 pp.
- Spangenberg, E., U. Spangenberg, and C. Heindorf (1998), "An experimental Study of Transport Properties of Porous Rock Salt," *Physics and Chemistry of the Earth*, 23, pp. 367-371.
- Spiers, C.J., and R.H. Brzesowsky (1993), *Densification Behaviour of Wet Granular Salt: Theory versus Experiment*. Seventh Symposium on Salt Vol. I. Elsevier Science Publishers B.V., Amsterdam.
- Spiers, C.J., C.J. Peach, R.H. Brzesowsky, P.M.T.M. Schutjens, J.L. Liezenberg, and H.J. Zwart (1988), *Long-term Rheological and Transport Properties of Dry and Wet Salt Rocks*. Commission of the European Communities, Directorate-General Science, Research and Development, EUR 11848 EN, ISBN 92-825-9191-3.
- Spiers, C.J., P.M.T.M. Schutjens, R.H. Brzesowsky, C.H. Peach, J.L. Liezenberg, and H.J. Zwart (1990), *Experimental Determination of Constitutive Parameters Governing Creep of Rocksalt by Pressure Solution*. In: R.J. Knipe and E.H. Rutter (Editors), *Deformation Mechanisms, Rheology and Tectonics*. Geol. Sci. Spec. Publ., 54.

Stormont, J.C., and J.J.K. Daemen (1992), "Laboratory study of gas permeability changes in rock salt during deformation," *Int. J. Rock Mech. Min. Sci. Geomech.*, Abstr., 29, pp. 325-342.

Stührenberg, D. (2004), Compaction and Permeability Behavior of Crushed Salt on Mixtures of Crushed Salt and Bentonite. Conference Proceedings of DisTec2004, International Conference on Radioactive Waste Disposal, Berlin, April 2004.

Stührenberg, D. (2007), Long-term laboratory investigation on backfill. – The Mechanical Behavior of Salt – Understanding of the THMC Processes in Salt, Proceedings of "Saltmech6" Hannover, Germany, Mai 2007, pp. 223–229.

Urai, J.L., W.D. Means, and G.S. Lister (1986a), Dynamic recrystallization of minerals. In: Mineral and rock deformation; laboratory studies; the Paterson volume. AGU Geophysical Monograph (edited by B.E. Hobbs and H.C. Heard) 36, pp. 161-199.

Urai, J.L., C.J. Spiers., H.J. Zwart, and G.S. Lister (1986b), "Water weakening effects in rock salt during long term creep," *Nature* 324, pp. 554-557.

US Department of Energy (DOE) (2011), Geotechnical Analysis Report. March 2011. DOE/WIPP 11-3177, Carlsbad Field Office, Carlsbad, NM.

Warren, J.K. (2005), *Evaporites: sediments, resources and hydrocarbons*. Springer.

Wieczorek, K., and P. Schwarzianeck (2004), Untersuchung zur Auflockerungszone im Salinar (ALOHA2), Gesellschaft für Anlagen- und Reaktorsicherheit (GRS) mbH, GRS Bericht GRS 198.

Wieczorek, K., T. Rothfuchs, B. Förster, U. Heemann, S. Olivella, Chr. Lerch, A. Pudewills, P. Kamlot, J. Grupa, and K. Herchen (2009), THERESA Deliverable D9, Coupled Processes in Salt Host-Rock Repositories - Final Report of Work Package 3, Coordinated by Gesellschaft für Anlagen- und Reaktorsicherheit (GRS) mbH, Braunschweig, 30 November 2009.

Zhang, C.L., M.W. Schmidt, G. Staupendahl, and U. Heemann (1993), Entwicklung eines Stoffansatzes zur Beschreibung des Kompaktionsverhaltens von Salzgrus. Bericht Nr. 93 -73 aus dem Institut für Statik der Technischen Universität Braunschweig.